

A Graph-Based Modeling Abstraction for Optimization: Concepts and Implementation in Plasmo.jl

Jordan Jalving · Sungho Shin · Victor M. Zavala

Abstract We present a general graph-based modeling abstraction for optimization that we call an *OptiGraph*. Under this abstraction, *any* optimization problem is treated as a hierarchical hypergraph in which nodes represent optimization subproblems and edges represent connectivity between such subproblems. The abstraction enables the modular construction of highly complex models in an intuitive manner, facilitates the use of graph analysis tools (to perform partitioning, aggregation, and visualization tasks), and facilitates communication of structures to decomposition algorithms. We provide an open-source implementation of the abstraction in the `Julia`-based package `Plasmo.jl`. We provide tutorial examples and large application case studies to illustrate the capabilities.

Keywords: graph theory, optimization, modeling, structure, decomposition

1 Motivation and Background

Advances in decomposition *algorithms* and *computing architectures* are continuously expanding the complexity and scale of optimization models that can be tackled [42]. Application examples include financial planning [25], supply chain scheduling [52], enterprise-wide management [28],

✉

Jordan Jalving
jalving@wisc.edu

Sungho Shin
sungho.shin@wisc.edu

Victor M. Zavala
victor.zavala@wisc.edu

Department of Chemical and Biological Engineering
University of Wisconsin-Madison, 1415 Engineering Dr, Madison, WI 53706, USA

infrastructure optimization [43], and network control [61]. Decomposition algorithms seek to address computational bottlenecks (in terms of memory, robustness, and speed) by exploiting structures present in a model [65, 83, 9, 16, 11]. Well-known algorithms to exploit structures at the problem level include Lagrangian decomposition [22], Benders decomposition [64], Dantzig-Wolfe decomposition [6], progressive hedging [81], Gauss-Seidel [72], and the alternating direction method of multipliers [8]. Fundamentally, these algorithms seek to solve the original problem by solving subproblems defined over *subproblem partitions* and by coordinating subproblem solutions via communication of primal-dual information. Well-known paradigms to exploit structures at the linear-algebra level (inside optimization solvers) include block elimination and preconditioning (e.g., Schur and Riccati) [26, 42, 63, 60]. In these schemes, the original problem is solved by using a general algorithm (e.g., interior-point, sequential quadratic programming, or augmented Lagrangian) and decomposition occurs during the computation of the search step.

The efficient use of decomposition algorithms (and of computing architectures under which they are executed) relies on the ability to communicate model structures in a *flexible* manner. Surprisingly, the development of *modeling environments* that support the development of decomposition algorithms has remained rather limited. As a result, decomposition algorithms have been mostly used to tackle models that have rather obvious structures such as stochastic optimization [49, 47, 75, 50, 35], network optimization [71], dynamic optimization [7], and hierarchical optimization [27]. Some examples of environments that support structured modeling include the structure-conveying modeling language (SML) [15], which is an extension of AMPL [23] that conveys structures in the form of variable and constraint blocks. SML was one of the earliest attempts to automate structure identification and exploitation in modeling environments and was motivated by the availability of structure-exploiting interior point solvers. `Pyomo` [32] is a *Python*-based modeling package that enables the expression of structures in the form of variable and constraint blocks. `Pyomo` also provides a structured modeling template called `PySP` [81] that greatly facilitates the expression of multi-stage stochastic programs and their solution using progressive hedging and Benders decomposition. `StuctJuMP` [36] and `StochasticPrograms.jl` [7] are extensions of the *Julia*-based package `JuMP.jl` [19] to express stochastic optimization structures.

1.1 Graph-Based Model Representations

It is important to recall that, at a fundamental level, an optimization model is a collection of algebraic functions (constraints and objectives) that are connected via variables. Connectivity between functions and variables can be represented as *graphs*. This concept is by no means new; graph representations of optimization models are routinely used in modeling environments to perform automatic differentiation and model processing tasks [23]. The underlying graph structure of the model is also implicitly communicated to solvers in the form of sparsity patterns of constraint, objective, and derivative matrices. However, these graph representations operate at a level of granularity that might not be particularly useful for decomposition. Specifically, the benefits of decomposition tend to become apparent when operating over *blocks* of functions and variables. An issue that arises here is that identifying blocks that are suitable for a decomposition algorithm and computing architecture is not an easy task. For instance, we might want to identify blocks that have sparse external connectivity (to reduce the amount of inter-block coupling) [63]. Moreover, if decomposition is to be executed on a parallel computer, one might want to ensure that the blocks are of similar size (to avoid load imbalance issues) [46]. Another issue that arises here is

that blocks might be *degenerate* (e.g., they might have more constraints than variables). Existing modeling environments do not provide capabilities to handle such issues.

To highlight some of the challenges that arise in the modeling structured problems, consider the natural gas network depicted in the left panel of Figure 1a. This is a regional gas transmission system that contains 215 pipelines, 16 compressors, 172 junction points [13]. The problem has an obvious structure induced by the network topology. This representation naturally conveys connectivity between components (pipelines, compressors, and junctions). Hidden in this representation, however, is the internal connectivity present in such components; this inner connectivity is usually complex and induced by variables and constraints that capture physical coupling (e.g., conservation of mass, energy, and momentum). The issue here is that there is a severe imbalance in the complexity of the components (e.g, pipelines might contain partial differential equations to capture flow while compressors contain much simpler algebraic equations). Moreover, hidden in the representation is the connectivity of the components across *time*, which gives rise to complex space-time coupling. Intuitively, one could seek to decompose the model *spatially* by exploiting the network topology, as shown in the middle panel of Figure 1b. Unfortunately, this approach does not account for inner component complexity and results in partitions with a disparate number of variables and constraints. This will give rise to load balancing issues and limit the benefits of parallel computation. To deal with this issue, one could seek to decompose the problem *temporally*, as shown in the right panel of Figure 1c. This approach leads to well-balanced partitions (every partition is a copy of the network), but leads to significantly more coupling between partitions. A high degree of coupling will also limit the scalability of algorithms (increased coupling tends to increase communication and slow down convergence). One would intuitively expect that there exist partitions that can balance coupling and load balancing (by traversing space-time and exploiting inner block complexity). Identifying such partitions, however, requires *unfolding* of the model structure. Figure 2a provides a visual rendering of the spatial representation of the natural gas system that unfolds inner component connectivity. Here, the size of the clusters gives us an initial indication of component complexity. Figure 2b is a visual rendering of the space-time representation that further unfolds temporal connectivity between components and this clearly reveals interesting (but complex) structures. Determining effective partitions from such structures requires advanced graph partitioning techniques.

So the question is: *If an optimization model is a graph after all, why is it that we do not use graph concepts to build optimization models?* Most optimization modelers follow an algebraic modeling paradigm in which the model is assembled by adding functions and variables (e.g., using packages such as GAMS, AMPL, Pyomo). There is, however, another modeling paradigm known as object-oriented modeling, in which the model is assembled by adding blocks of functions and variables. This paradigm is widely used in engineering communities to perform simulation (e.g., using packages such as Modelica, AspenPlus, and gProms [53,18]). An important observation is that object-oriented modeling more naturally lends itself to the expression and exploitation of problem structures because the underlying graph is progressively built by the user. For instance, packages such as AspenPlus use the underlying graph structure induced by blocks to partition the model and communicate it to a decomposition algorithm. One could thus think of object-oriented modeling as a form of graph-based modeling. The purely object-oriented paradigm however, may suffer from imbalance of component complexity or from a high degree of coupling when performing decomposition.

Recently, we proposed a graph-based abstraction to build optimization models [37,38]. In this abstraction, any optimization model is treated as a *hierarchical graph*. At a given level, a graph

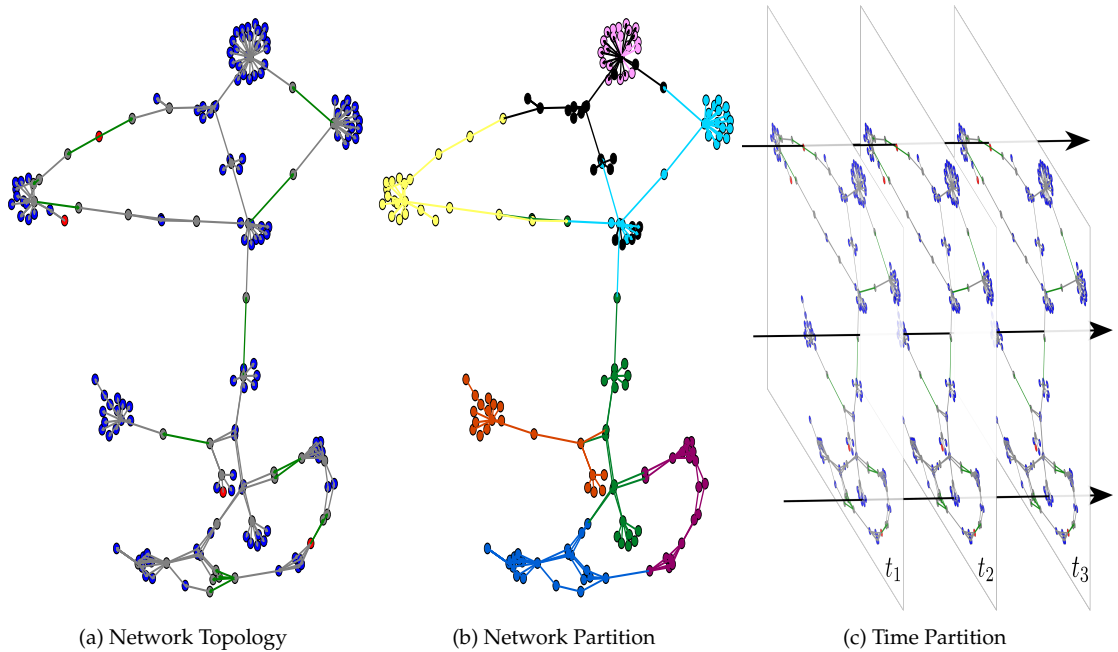


Fig. 1: Natural gas transmission network and possible partitioning strategies. The network layout of the system (left)), the system split into eight network partitions (middle), and the system represented by three time partitions (right).

comprises a set of nodes and edges; each node contains an optimization model (with variables, objectives, constraints, and data) and each edge captures connectivity between node models. Importantly, the optimization model in each node can be expressed algebraically (as in a standard algebraic modeling language) or as a graph (thus enabling inheritance and creation of hierarchical graphs). This provides flexibility to capture both algebraic and object-oriented modeling paradigms under the same framework. The abstraction naturally exposes problem structure to algorithms and provides a modular approach to construct models. Modularization enables collaborative model building, independent processing of model components (e.g., automatic differentiation), and data management. The abstraction naturally captures a wide range of problem classes such as stochastic optimization (graph is a tree), dynamic optimization (graph is a line), network (graph is the network itself), PDE optimization (graph is a mesh), and multiscale optimization (graph is a meshed tree). Moreover, graphs can be naturally built by combining graphs from different classes (e.g., stochastic PDE optimization). This approach is thus more general than other graph-based abstractions proposed for specific problem classes such as network optimization and control [33,41,55,78,31]. This modeling abstraction also generalizes those used in simulation packages such as *Modelica*, *AspenPlus*, *gProms*, which are tailored to specific physical systems. The hierarchical graph structure can be communicated to decomposition solvers or it can be collapsed into an optimization model that can be solved with off-the-shelf solvers (e.g., *Gurobi* or *Ipopt*). To illustrate the types of capabilities enabled by hierarchical graph modeling, we take the natural-gas network in Figure 1a and couple it to an electrical network, as shown in Figure 3a. Here, the

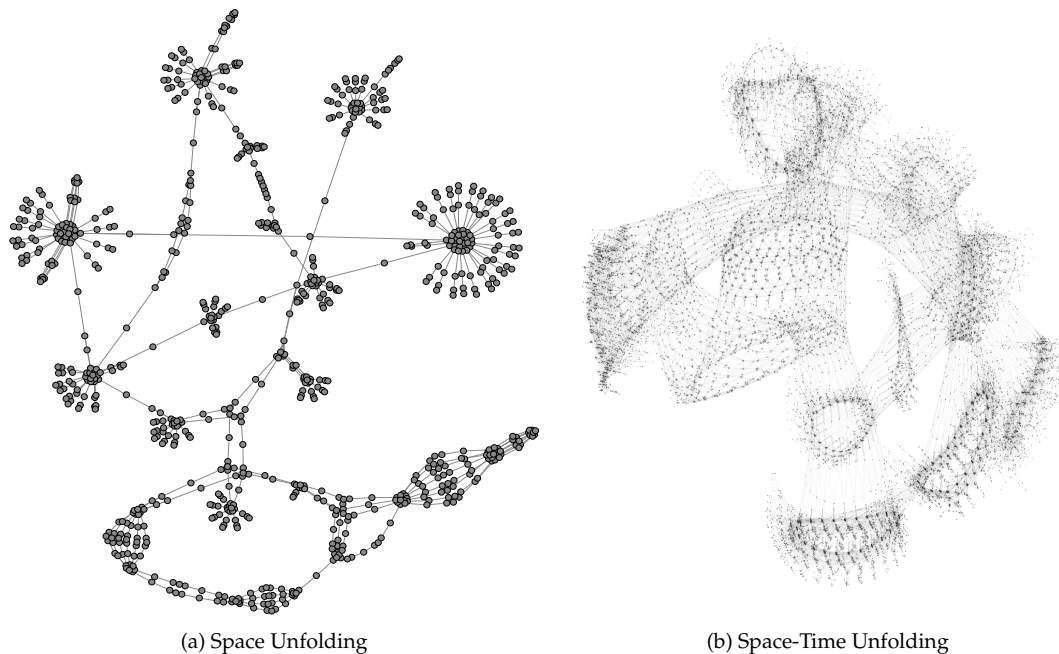


Fig. 2: Space and space-time unfolding of natural gas network (uncovering components).

natural gas graph and the electrical power graph can be built independently and then coupled to construct a higher level graph. The graph structure can be communicated to a graph visualization tool and this allows us to analyze the graph using different representations. In the left panel we see a traditional representation of infrastructure coupling (that hides temporal and component coupling), while in the middle and right panels we unfold spatial and spatio-temporal coupling. The space-time graph contains over 100,000 nodes and 300,000 edges and reveals that there exist a large number of non-obvious structures that might be beneficial from a computational standpoint.

Graph-based model representations can take advantage of powerful graph *analysis* tools. For instance, graph partitioning tools such as *Metis* [44] and *Scotch* [59] provide efficient algorithms to automatically analyze problem structure and to identify suitable partitions to be exploited by decomposition algorithms. Graph partitioning seeks to decompose a domain described by a graph such that communication between subdomains is minimized subject to load balancing (i.e., the domains are about the same size). The most ubiquitous graph partitioning applications target parallelizing scientific simulations [67], performing sparse-matrix operations [30], and preconditioning systems of PDEs [68]. Hypergraph partitioning generalizes graph partitioning concepts to effectively decompose non-symmetric domains [17] and has been applied to physical network design and sparse-matrix-vector multiplication [58]. Popular hypergraph partitioning tools include *hMetis* [45] and *PaToH* [12]. Community detection approaches have also been used to find partitions that maximize modularity [56,2]. Graph partitioning approaches have been used to decompose optimization problems in various contexts. Graph approaches have been used to partition network optimization problems using graph coloring techniques [84] and block partitioning schemes [85]. Bipartite graph representations have been used to permute linear programs [21] into

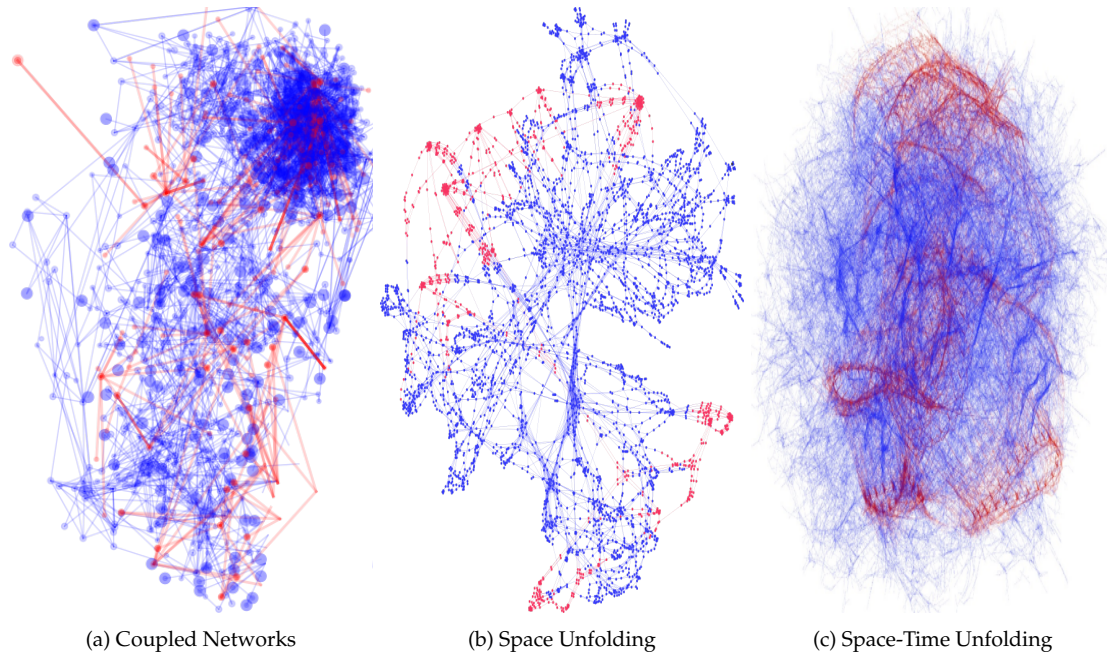


Fig. 3: Network topology of coupled natural gas (in blue) and electric (in red) networks (left), space unfolding of components (middle), and space-time unfolding of components (right).

block diagonal form to enable parallel solution. Hypergraph partitioning has been used to decompose mixed-integer programs to formulate Dantzig-Wolfe decompositions [80,6] using `hMetis` and `PaToH`. Community detection approaches have been used to automate structure identification in general optimization problems and with this enable higher efficiency of decomposition algorithms [77,2]. We highlight that these approaches start with a given algebraic optimization model that is then transformed into a graph representation; consequently, these are not graph modeling abstractions *per se*.

Graph-based representations have been adopted in *modeling environments* for specific problem classes. `SnapVX` [31] uses a graph topology abstraction to formulate network optimization problems that are solved using ADMM [8]. `GRAVITY` [34] is an algebraic modeling framework that incorporates graph-aware modeling syntax but this is not the paradigm driving the environment. `DISROPT` is a `Python`-based environment for distributed network optimization [20]. `DeCODE` [3] is a package written in `Matlab` and `Python` that automatically creates a bipartite representation of optimization models created with `Pyomo` and uses community detection to determine partitions for use with `Benders` or `Lagrangian` decomposition. In recent work we have provided a `Julia`-based implementation of our hierarchical graph abstraction, that we called `Plasmo.jl` [37,38]. This package provides modeling syntax to systematically create hierarchical graph models, to integrate algebraic `JuMP.jl` [19] models within nodes, and to facilitate the expression of connectivity between node models. The first version of `Plasmo.jl` used an abstraction that was targeted to handle coupled infrastructure networks. This abstraction sought to generalize the network modeling capabilities of `DMNetwork` [1] (used for simulation) to handle optimization problems [37].

Subsequent development provided data management capabilities to facilitate model reduction and re-use (for real-time optimization applications) [39] and provided an interface to communicate graph structures to the parallel interior-point solver `PIPS-NLP` [10]. The abstraction was later used to create a `computational graph` abstraction wherein nodes are computational tasks and edges communicate data between tasks. This abstraction enables hierarchical modeling of cyber-physical systems, workflows, and algorithms [38].

1.2 Contributions of This Work

In this work, we present a new and general graph modeling abstraction for optimization that we call an `OptiGraph`. As in our previously proposed abstraction, we represent any optimization model as a hierarchical graph wherein nodes contain optimization models with corresponding objectives, variables, constraints, and data. The novel feature of our abstraction lies on how *edge connectivity* between models is represented. Specifically, we express connectivity in the form of *hyperedges* (edges that can connect multiple nodes), thus generalizing the concept of an edge (which connects two nodes). This hypergraph representation enables a more intuitive expression of structures at the modeling level and enables the use of efficient hypergraph analysis tools. The hypergraph representation can also be transformed into a standard graph representation (via lifting) and to other graph representations (e.g., bipartite) and this enables the use of different graph analysis techniques and tools and enables flexible expression of structures for decomposition. We provide an efficient implementation of the `OptiGraph` abstraction in `Plasmo.jl` that can handle hundreds of thousands to millions of nodes and edges. We implement an interface to `LightGraphs.jl` and `Gephi` to demonstrate that the implementation facilitates interfacing to graph analysis and visualization tools [69,5]. We illustrate how to use these tools and topological information obtained from the `OptiGraph` to automatically obtain partitions that trade-off coupling and load balancing and to compute useful descriptors of the graph (e.g., neighborhoods, degree distribution, minimum spanning tree, modularity). Moreover, we show how to manipulate the graph to perform aggregation functions (merge nodes). These features provide flexibility to visualize, decompose, and solve large models using different techniques. We implement an interface to the parallel solver `PIPS-NLP` to analyze computational efficiency obtained with different partitioning strategies. We also demonstrate that the abstraction facilitates the implementation of decomposition algorithms; to do so, we implement an overlapping Schwarz scheme that is tailored to graph-structured problems [74].

1.3 Paper Structure

The rest of the paper is organized as follows: Section 2 describes the `OptiGraph` abstraction and its implementation in `Plasmo.jl`. In Section 3 we show how the `OptiGraph` structure can be exploited by different optimization algorithms. Section 4 provides case studies that demonstrate capabilities on a large natural gas network problem and on a direct current optimal power flow (DC OPF) problem. Section 5 concludes the manuscript and discusses future directions for `Plasmo.jl`.

2 Hierarchical Graph Abstraction and Implementation

This section introduces the `OptiGraph` abstraction alongside its implementation in `Plasmo.jl`. In a nutshell, `Plasmo.jl` is a graph-structured modeling language that offers concise syntax and access to graph tools that enable model analysis and manipulation (e.g., partitioning, aggregation, visualization). `Plasmo.jl` is an official Julia package hosted at <https://github.com/zavalab/Plasmo.jl>. All example scripts in this section can be found at <https://github.com/zavalab/JuliaBox/tree/master/PlasmoExamples>.

2.1 Graph Abstraction

The `OptiGraph` abstraction proposed is composed of a set of *OptiNodes* \mathcal{N} (each embedding an optimization model with its local variables, constraints, objective function, and data) and a set of *OptiEdges* \mathcal{E} (each embedding a set of *linking constraints*) that capture coupling between *OptiNodes*. The `OptiGraph` is denoted as $\mathcal{G}(\mathcal{N}, \mathcal{E})$ and contains the optimization model of interest. The `OptiEdges` \mathcal{E} are hyperedges that connect two or more `OptiNodes`. The `OptiGraph` is an undirected hypergraph. Whenever clear from context, we simply refer to the `OptiGraph` as graph, to the `OptiNodes` as nodes, and to *OptiEdges* as edges. We denote the set of nodes that belong to \mathcal{G} as $\mathcal{N}(\mathcal{G})$ and the set of edges as $\mathcal{E}(\mathcal{G})$. The topology of the hypergraph is encoded in the incidence matrix $A \in \mathcal{R}^{|\mathcal{N}| \times |\mathcal{E}|}$; here, the notation $|\mathcal{S}|$ denotes cardinality of set \mathcal{S} . The neighborhood of node n is denoted as $\mathcal{N}(n)$ and this is the set of nodes connected to n . The set of nodes that support an edge e are denoted as $\mathcal{N}(e)$ and the set of edges that are incident to node n are denoted as $\mathcal{E}(n)$.

The optimization model associated with an `OptiGraph` can be represented mathematically as:

$$\min_{\{x_n\}_{n \in \mathcal{N}(\mathcal{G})}} \sum_{n \in \mathcal{N}(\mathcal{G})} f_n(x_n) \quad (\text{Objective}) \quad (2.1a)$$

$$\text{s.t. } x_n \in \mathcal{X}_n, \quad n \in \mathcal{N}(\mathcal{G}), \quad (\text{Node Constraints}) \quad (2.1b)$$

$$g_e(\{x_n\}_{n \in \mathcal{N}(e)}) = 0, \quad e \in \mathcal{E}(\mathcal{G}). \quad (\text{Link Constraints}) \quad (2.1c)$$

Here, $\{x_n\}_{n \in \mathcal{N}(\mathcal{G})}$ is the collection of decision variables over the entire set of nodes $\mathcal{N}(\mathcal{G})$ and x_n is the set of variables on node n . Function (2.1a) is the graph objective function which is given by the sum of objective functions $f_n(x_n)$, (2.1b) represents the collection of constraints over all nodes $\mathcal{N}(\mathcal{G})$, and (2.1c) is the collection of linking constraints over all edges $\mathcal{E}(\mathcal{G})$. Here, the constraints of a node n are represented by the set \mathcal{X}_n while the linking constraints induced by an edge e are represented by the vector function $g_e(\{x_n\}_{n \in \mathcal{N}(e)})$ (an edge can contain multiple linking constraints). The optimization problem representation captures sufficient features to facilitate the discussion but differs from the actual implementation. For example, here we assume that the graph objective is obtained via a linear combination of the node objectives but other combinations are possible (e.g., to handle conflict resolution formulations wherein nodes represent different stakeholders). In addition, we assume that coupling between nodes arises in the form of complicating constraints but definition of complicating variables is also possible (coupling variables can always be represented as coupling constraints via lifting).

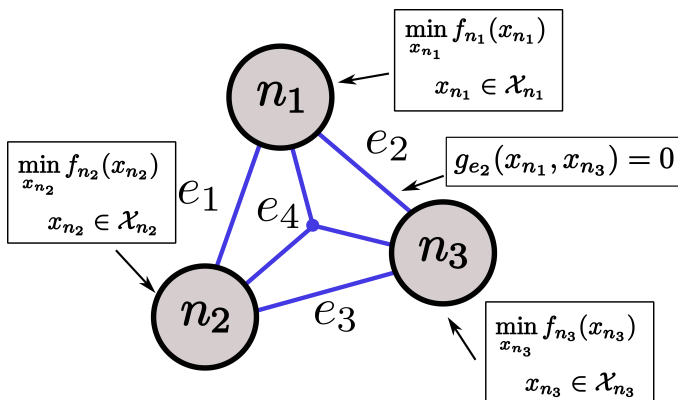


Fig. 4: OptiGraph with three OptiNodes connected by four OptiEdges

2.2 Syntax and Usage

We now introduce the `Plasmo.jl` implementation of the `OptiGraph` and show how to use its syntax to create, analyze, and solve an optimization model. `Plasmo.jl` implements the graph model described by (2.1) and illustrated in Figure 4. In our implementation, an `OptiNode` encapsulates a `Model` object from the `JuMP.jl` modeling language. This harnesses the algebraic modeling syntax and processing functionality of `JuMP.jl`. An `OptiEdge` object encapsulates the linking constraints that define coupling between the nodes.

2.2.1 Example 1 : Creating an OptiGraph

We start with the simple example given by (2.2) to demonstrate `OptiGraph` syntax:

$$\min \quad y_{n_1} + y_{n_2} + y_{n_3} \quad (\text{Objective}) \quad (2.2a)$$

$$\text{s.t.} \quad x_{n_1} \geq 0, y_{n_1} \geq 2, x_{n_1} + y_{n_1} \geq 3 \quad (\text{Node 1 Constraints}) \quad (2.2b)$$

$$x_{n_2} \geq 0, x_{n_2} + y_{n_2} \geq 3 \quad (\text{Node 2 Constraints}) \quad (2.2c)$$

$$x_{n_3} \geq 0, x_{n_3} + y_{n_3} \geq 3 \quad (\text{Node 3 Constraints}) \quad (2.2d)$$

$$x_{n_1} + x_{n_2} + x_{n_3} = 3 \quad (\text{Link Constraint}) \quad (2.2e)$$

In this model, equations (2.2b), (2.2c), and (2.2d) represent individual node constraints and (2.2e) is a linking constraint that couples the three nodes. We formulate and solve this optimization model as shown in Snippet 1. We import `Plasmo.jl` into a `Julia` session on Line 1 as well as the off-the-shelf linear programming solver `GLPK` [51] to solve the problem. We define `graph1` (an `OptiGraph`) on Line 5 and then create three `OptiNodes` on Lines 8-24 using the `@optinode` macro. We also use the `@variable`, `@constraint`, and `@objective` macros (extended from `JuMP.jl`) to define node model attributes. Next, we use the `@linkconstraint` macro on Line 27 to create a linking constraint between the three nodes. Importantly, this *automatically* creates an `OptiEdge`. This feature is key, as the user does not need to express the topology of the graph (this is automatically created behind the scenes as linking constraints are added). In other words,

the user does not need to provide an adjacency matrix (which can be highly complex). We solve the problem using the GLPK optimizer on Line 30. Since GLPK does not exploit graph structure, `Plasmo.jl` automatically transforms the graph into a standard LP format. We query the solution for each variable using the `value` function on Line 33 which accepts the corresponding node and variable we wish to query. Another important feature is that the solution data retains the structure of the `OptiGraph`, and this facilitates query and analysis. We also highlight that the syntax is similar to that of `JuMP.jl` but operates at a higher level of abstraction.

We have implemented capabilities to visualize the structure of `OptiGraphs` by extending plotting functions available in `Plots.jl`. We layout the `OptiGraph` topology on Line 39 using the `plot` function and we plot the underlying adjacency matrix structure on Line 44 using the `spy` function. Both of these functions can accept keyword arguments to customize their layout or appearance. The matrix visualization also encodes information on the number of variables and constraints in each node and edge. The results are depicted in Figure 5; the left figure shows a standard graph visualization where we draw an edge between each pair of nodes if they share an edge, and the right figure shows the matrix representation where labeled blocks correspond to nodes and blue marks represent linking constraints that connect their variables. The node layout helps visualize the overall connectivity of the graph while the matrix layout helps visualize the size of nodes and edges.

2.3 Hierarchical Graphs

A key novelty of the `OptiGraph` abstraction is that it can cleanly represent hierarchical structures. This feature enables expression of models with multiple embedded structures and enables modular model building (e.g., by merging existing models). To illustrate this, consider you have the `OptiGraphs` $\mathcal{G}_i, \mathcal{G}_j$ each with its own local nodes and edges. We assemble these low-level `OptiGraphs` (subgraphs) to build a high-level `OptiGraph` $\mathcal{G}(\{\mathcal{G}_i, \mathcal{G}_j\}, \mathcal{N}_g, \mathcal{E}_g)$. We use the notation $\mathcal{G}(\mathcal{N}, \mathcal{E})$ to indicate that the high-level graph has nodes $\mathcal{N} = \mathcal{N}_g \cup \mathcal{N}(\mathcal{G}_i) \cup \mathcal{N}(\mathcal{G}_j)$ and edges $\mathcal{E} = \mathcal{E}_g \cup \mathcal{E}(\mathcal{G}_i) \cup \mathcal{E}(\mathcal{G}_j)$. Here, \mathcal{E}_g are global edges in \mathcal{G} (connect nodes across low-level graphs $\mathcal{G}_i, \mathcal{G}_j$ but are not elements of such subgraphs) and \mathcal{N}_g are global nodes in \mathcal{G} (can be connected to nodes in low-level graphs but that are not elements of such subgraphs). For every global edge $e \in \mathcal{E}_g$, we have that $\mathcal{N}(e) \in \mathcal{N}(\mathcal{G}_i), \mathcal{N}(\mathcal{G}_j)$, and \mathcal{N}_g where $\mathcal{N}(\mathcal{G}_i) \cap \mathcal{N}(\mathcal{G}_j) \cap \mathcal{N}_g = \emptyset$. In other words, the edges \mathcal{E}_g only connect nodes across low-level graphs \mathcal{G}_i and \mathcal{G}_j or between global nodes \mathcal{N}_g in \mathcal{G} and low-level graphs. Consequently, if we treat the elements of a node set \mathcal{N} as a graph (i.e., we combine subgraphs into a single `OptiNode`), we can represent $\mathcal{G}(\{\mathcal{G}_i, \mathcal{G}_j\}, \mathcal{E}_g, \mathcal{N}_g)$ as $\mathcal{G}(\mathcal{N}, \mathcal{E})$. This nesting procedure can be carried over multiple levels to form a hierarchical graph.

The formulation given by (2.1) can be extended to describe a hierarchical graph with an arbitrary number of subgraphs. This is shown in (2.3); here, $\{x_n\}_{n \in \mathcal{N}(\mathcal{G})}$ represents the collection of variables over the entire set of nodes in the graph. Equation (2.3c) are the linking constraints over the edges for each subgraph. Here, we use the notation $\mathcal{SG} \in \mathcal{AG}(\mathcal{G})$ to indicate that the subgraph elements \mathcal{SG} are part of the recursive set of subgraphs in \mathcal{G} (i.e., set contains all subgraphs in the graph). Specifically, we define the mapping $\mathcal{AG} : \mathcal{G} \rightarrow \{\mathcal{SG}_1, \mathcal{SG}_2, \mathcal{SG}_3, \dots, \mathcal{SG}_N\}$ where N is the total number of subgraphs in \mathcal{G} .

Code Snippet 1: Creating and Solving an OptiGraph in Plasmojl

```

1  using Plasmojl
2  using GLPK
3  using Plots
4
5  graph1 = OptiGraph()
6
7  #Create three OptiNodes
8  @optinode(graph1,n1)
9  @variable(n1, y >= 2)
10 @variable(n1,x >= 0)
11 @constraint(n1,x + y >= 3)
12 @objective(n1, Min, y)
13
14 @optinode(graph1,n2)
15 @variable(n2, y)
16 @variable(n2,x >= 0)
17 @constraint(n2,x + y >= 3)
18 @objective(n2, Min, y)
19
20 @optinode(graph1,n3)
21 @variable(n3, y)
22 @variable(n3,x >= 0)
23 @constraint(n3,x + y >= 3)
24 @objective(n3, Min, y)
25
26 #Create link constraint between nodes (automatically creates an optiedge on graph1)
27 @linkconstraint(graph1, n1[:x] + n2[:x] + n3[:x] == 3)
28
29 #Optimize with GLPK
30 optimize!(graph1,GLPK.Optimizer)
31
32 #Query Solution
33 value(n1,n1[:x])
34 value(n2,n2[:x])
35 value(n3,n3[:x])
36 objective_value(graph1)
37
38 #Visualize graph topology
39 plt_graph1 = Plots.plot(graph1,node_labels = true,
40 markersize = 60,labels = 30, linewidth = 4,
41 layout_options = Dict(:tol => 0.01,:iterations => 2));
42
43 #Visualize graph adjacency
44 plt_matrix1 = Plots.spy(graph1,node_labels = true,markersize = 30);

```

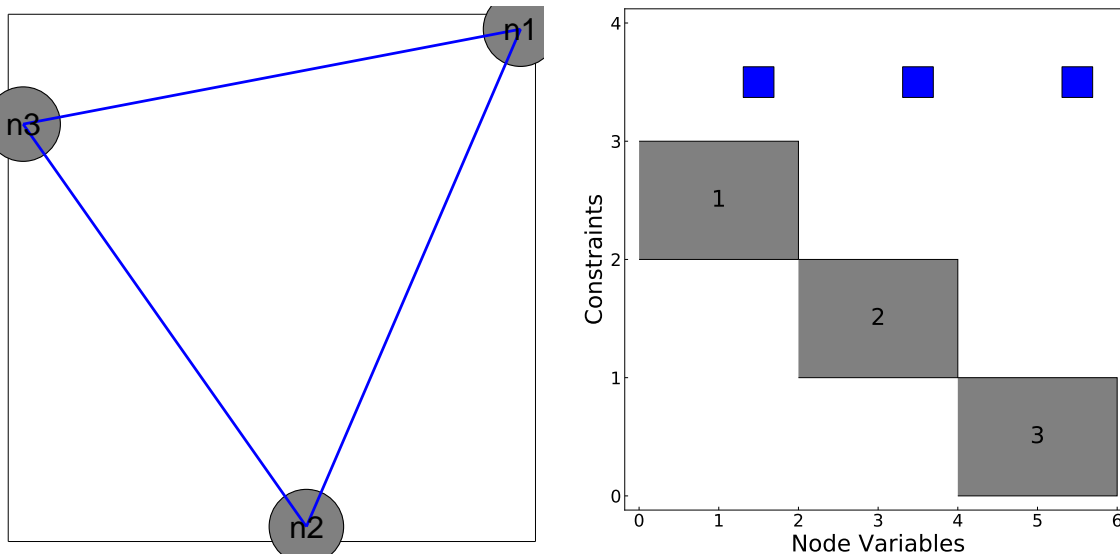


Fig. 5: Output visuals for Code Snippet 1. Graph topology obtained with `plot` function (left) and graph matrix representation obtained with `spy` function (right).

$$\min_{\{x_n\}_{n \in \mathcal{N}}} \sum_{\mathcal{SG} \in \mathcal{AG}(\mathcal{G})} \sum_{n \in \mathcal{N}(\mathcal{SG})} f_n(x_n) \quad (\text{Objective}) \quad (2.3a)$$

$$\text{s.t. } x_n \in \mathcal{X}_n, \quad n \in \mathcal{N}(\mathcal{SG}), \mathcal{SG} \in \mathcal{AG}(\mathcal{G}) \quad (\text{Node Constraints}) \quad (2.3b)$$

$$g_e(\{x_n\}_{n \in \mathcal{N}(e)}), e \in \mathcal{E}(\mathcal{SG}), \mathcal{SG} \in \mathcal{AG}(\mathcal{G}) \quad (\text{Subgraph Link Constraints}) \quad (2.3c)$$

$$g_e(\{x_n\}_{n \in \mathcal{N}(e)}), e \in \mathcal{E}(\mathcal{G}). \quad (\text{Graph Link Constraints}) \quad (2.3d)$$

Figures 6 and 7 depict examples of graphs with subgraph nodes. In Figure 6 we have a graph \mathcal{G} that contains three subgraphs $\mathcal{SG}_1, \mathcal{SG}_2, \mathcal{SG}_3$ with a total of nine nodes (three in each subgraph). The graph \mathcal{G} contains a global hyperedge that connects to local nodes in the subgraphs. Figure 7 shows a hierarchical graph \mathcal{G} with three subgraphs $\mathcal{SG}_1, \mathcal{SG}_2, \mathcal{SG}_3$ and nine total nodes. The graph \mathcal{G} contains a global node n_0 that is connected to nodes in the subgraphs. This type of structure arises when there is a parent (master) optimization problem that is connected to children subproblems.

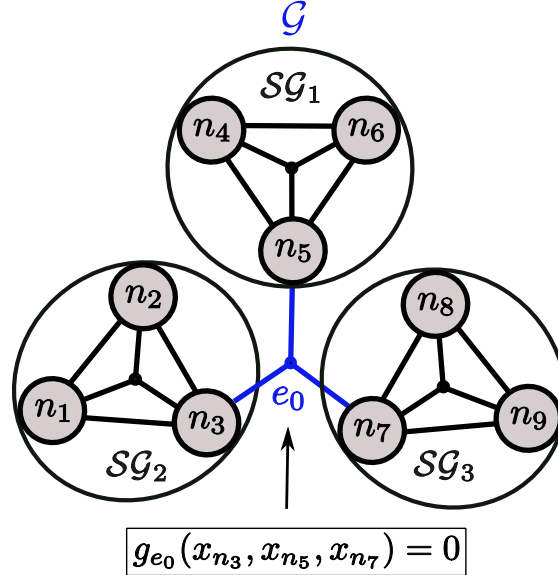


Fig. 6: An OptiGraph that contains three subgraphs. The subgraphs are coupled through the global edge e_0 in OptiGraph \mathcal{G} .

2.3.1 Example 2: Hierarchical Graph with Global Edge

An OptiGraph object manages its own nodes and edge in a *self-contained* manner (without requiring references to other higher-level graphs). Consequently, we can define subgraphs independently (in a modular manner) and these can be coupled together by using global edges or nodes

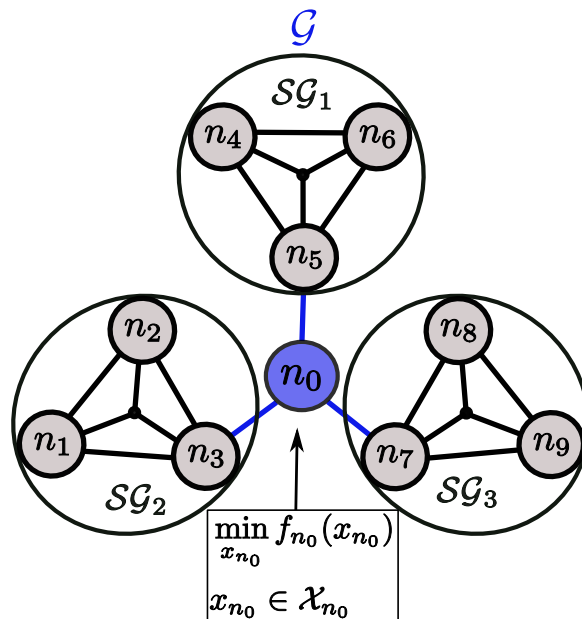


Fig. 7: An OptiGraph that contains three subgraphs. The subgraphs are coupled to the global node n_0 in OptiGraph \mathcal{G} .

defined on a high-level graph. This feature is key because each node can have its own syntax (syntax does not need to be consistent or non-redundant over the entire model). This is a fundamental difference with algebraic modeling languages (syntax has to be consistent and non-redundant over the entire model). The formulation in (2.4) illustrates how to express hierarchical connectivity using a global edge. Equation (2.4a) is the summation of every node objective function in the graph; (2.4b), (2.4c) and (2.4d) describe node constraints; (2.4e), (2.4f), and (2.4g) represent link constraints within each subgraph; and (2.4h) defines a link constraint at the higher level graph (that links nodes from each individual subgraph). Formulation (2.4) can be expressed as a hierarchical OptiGraph using the `add_subgraph!` function. This functionality is shown in Code Snippet 2, where we extend `graph1` from Code Snippet 1. We create a new graph called `graph2` on Line 2 and setup nodes and link them together on Lines 4 through 17. We also construct `graph3` in the same fashion on Lines 20 through 35. Next, we create `graph0` on Line 38 and add graphs `graph1`, `graph2`, and `graph3` as subgraphs to `graph0` on Lines 41 through 43. We add a linking constraint to `graph0` that couples nodes on each subgraph on Line 46 and solve the graph on Line 49. We present the graph visualization in Figure 8. Here we can see the hierarchical structure of the OptiGraph and the local and global coupling constraints. This structure is compatible with that shown in Figure 6.

$$\begin{aligned}
\min \sum_{i=1:9} y_{n_i} & && \text{(Node Objectives)} & (2.4a) \\
\text{s.t. } x_{n_i} \geq 0, y_{n_i} \geq 2, x_{n_i} + y_{n_i} \geq 3, i \in \{1, 2, 3\} & && \text{(Subgraph 1 Constraints)} & (2.4b) \\
x_{n_i} \geq 0, y_{n_i} \geq 2, x_{n_i} + y_{n_i} \geq 5, i \in \{4, 5, 6\} & && \text{(Subgraph 2 Constraints)} & (2.4c) \\
x_{n_i} \geq 0, y_{n_i} \geq 2, x_{n_i} + y_{n_i} \geq 7, i \in \{7, 8, 9\} & && \text{(Subgraph 3 Constraints)} & (2.4d) \\
x_{n_1} + x_{n_2} + x_{n_3} = 3 & && \text{(Subgraph 1 Link Constraint)} & (2.4e) \\
x_{n_4} + x_{n_5} + x_{n_6} = 5 & && \text{(Subgraph 2 Link Constraint)} & (2.4f) \\
x_{n_7} + x_{n_8} + x_{n_9} = 7 & && \text{(Subgraph 3 Link Constraint)} & (2.4g) \\
x_{n_3} + x_{n_5} + x_{n_7} = 10 & && \text{(Global Link Constraint)} & (2.4h)
\end{aligned}$$

2.3.2 Example 3: Hierarchical Graph with Global Node

We can express hierarchical connectivity within a `OptiGraph` by defining a global node that is connected with subgraph nodes. Formulation (2.5) illustrates this idea; this is analogous to (2.4) where we have removed the high level linking constraint (2.4h) and have replaced it with a high level node (2.5h) and three linking constraints that couple the graph to its subgraphs (2.5i). The implementation of the formulation in (2.5) is shown in Code Snippet 3. Here, we assume that we already have `graph1`, `graph2`, and `graph3` defined from Snippets 1 and 2. We recreate `graph0` and setup the node `n0` on Lines 2 through 7. We add subgraphs `graph1`, `graph2`, and `graph3` on Lines 10 through 12 like in the previous snippet, and add linking constraints that connect node `n0` to nodes in each subgraph on Lines 15 through 17. We solve the newly created `graph0` on Line 20 and present the visualization in Figure 9. This structure is compatible with that shown in Figure 7.

$$\begin{aligned}
\min \sum_{i=1:9} y_{n_i} & && \text{(Objective)} & (2.5a) \\
\text{s.t. } x_{n_i} \geq 0, y_{n_i} \geq 2, x_{n_i} + y_{n_i} \geq 3, i \in \{1, 2, 3\} & && \text{(Subgraph 1 Constraints)} & (2.5b) \\
x_{n_i} \geq 0, y_{n_i} \geq 2, x_{n_i} + y_{n_i} \geq 5, i \in \{4, 5, 6\} & && \text{(Subgraph 2 Constraints)} & (2.5c) \\
x_{n_i} \geq 0, y_{n_i} \geq 2, x_{n_i} + y_{n_i} \geq 7, i \in \{7, 8, 9\} & && \text{(Subgraph 3 Constraints)} & (2.5d) \\
x_{n_1} + x_{n_2} + x_{n_3} = 3 & && \text{(Subgraph 1 Link Constraint)} & (2.5e) \\
x_{n_4} + x_{n_5} + x_{n_6} = 5 & && \text{(Subgraph 2 Link Constraint)} & (2.5f) \\
x_{n_7} + x_{n_8} + x_{n_9} = 7 & && \text{(Subgraph 3 Link Constraint)} & (2.5g) \\
x_{n_0} \geq 0 & && \text{(Graph Constraint)} & (2.5h) \\
x_{n_0} + x_{n_3} = 3, x_{n_0} + x_{n_5} = 5, x_{n_0} + x_{n_7} = 7 & && \text{(Global Link Constraints)} & (2.5i)
\end{aligned}$$

2.4 Processing and Manipulating OptiGraphs

In addition to the graph construction functions presented in the previous examples (`@optinode`, `@linkconstraint`, `add_subgraph!`), it is also possible to query an `OptiGraph` object to retrieve its attributes. Table 1 summarizes the main `Plasmo.jl` functions used to create and inspect

Code Snippet 2: Hierarchical Connectivity using Global Edge

```

1  #Create low-level graph2
2  graph2 = OptiGraph()
3
4  @optinode(graph2,n4)
5  @variable(n4, x >= 0); @variable(n4, y >= 2)
6  @constraint(n4,x + y >= 5); @objective(n4, Min, y)
7
8  @optinode(graph2,n5)
9  @variable(n5, x >= 0); @variable(n5, y >= 2)
10 @constraint(n5,x + y >= 5); @objective(n5, Min, y)
11
12 @optinode(graph2,n6)
13 @variable(n6, x >= 0); @variable(n6, y >= 2)
14 @constraint(n6,x + y >= 5); @objective(n6, Min, y)
15
16 #Create graph2 linking constraint
17 @linkconstraint(graph2, n4[:x] + n5[:x] + n6[:x] == 5)
18
19 #Create low-level graph 3
20 graph3 = OptiGraph()
21
22 @optinode(graph3,n7)
23 @variable(n7, x >= 0); @variable(n7, y >= 2)
24 @constraint(n7,x + y >= 7); @objective(n7, Min, y)
25
26 @optinode(graph3,n8)
27 @variable(n8, x >= 0); @variable(n8, y >= 2)
28 @constraint(n8,x + y >= 7); @objective(n8, Min, y)
29
30 @optinode(graph3,n9)
31 @variable(n9, x >= 0); @variable(n9, y >= 2)
32 @constraint(n9,x + y >= 7); @objective(n9, Min, y)
33
34 #Create graph3 linking constraint
35 @linkconstraint(graph3, n7[:x] + n8[:x] + n9[:x] == 7)
36
37 #Create high-level graph0
38 graph0 = OptiGraph()
39
40 #Add subgraphs to graph0
41 add_subgraph!(graph0,graph1)
42 add_subgraph!(graph0,graph2)
43 add_subgraph!(graph0,graph3)
44
45 #Add linking constraint to graph0 connecting its subgraphs
46 @linkconstraint(graph0,n3[:x] + n5[:x] + n7[:x] == 10)
47
48 #Optimize with GLPK
49 optimize!(graph0,GLPK.Optimizer)

```

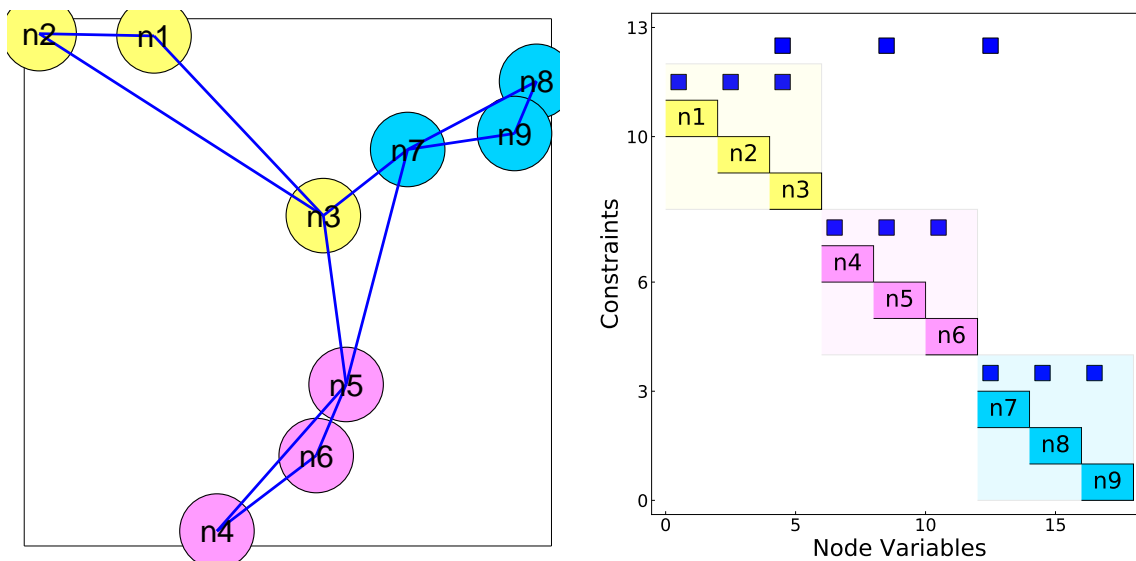


Fig. 8: Output visuals for Code Snippet 2 showing hierarchical structure of the `OptiGraph` with three subgraphs.

Code Snippet 3: Hierarchical Connectivity using Global Node

```

1 #Create graph0
2 graph0 = OptiGraph()
3
4 #Create a node on graph0
5 @optinode (graph0, n0)
6 @variable (n0, x)
7 @constraint (n0, x >= 0)
8
9 #Add subgraphs to graph0
10 add_subgraph! (graph0, graph1)
11 add_subgraph! (graph0, graph2)
12 add_subgraph! (graph0, graph3)
13
14 #Create linking constraints on graph0 connecting it to its subgraphs
15 @linkconstraint (graph0, n0[:x] + n3[:x] == 3)
16 @linkconstraint (graph0, n0[:x] + n5[:x] == 5)
17 @linkconstraint (graph0, n0[:x] + n7[:x] == 7)
18
19 #Optimize with GLPK
20 optimize! (graph0, GLPK.Optimizer)

```

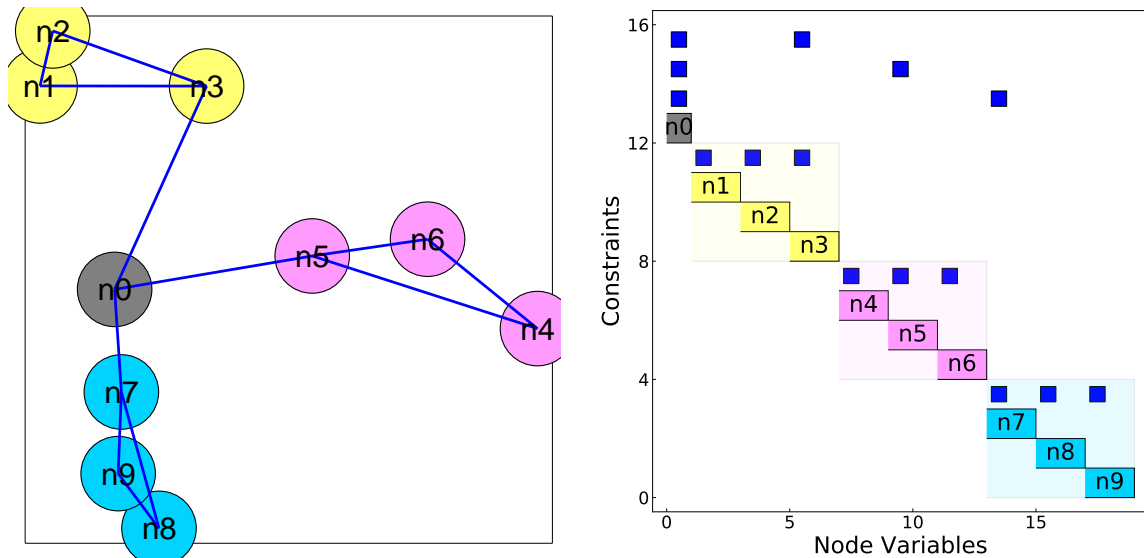


Fig. 9: Output visuals for Code Snippet 3 showing hierarchical structure of the `OptiGraph` with three subgraphs.

an `OptiGraph`. We inspect the nodes, edges, linking constraints, and subgraphs using `getoptinodes`, `getoptiedges`, `getlinkconstraints`, and `getsubgraphs` functions, and we can collect *all* of the corresponding graph attributes using recursive versions of these functions (`all_nodes`, `all_edges`, `all_linkconstraints` and `all_subgraphs`).

Thus far we have discussed how to enable model construction using a *bottom-up* approach. Specifically, we showed how to construct an `OptiGraph` by adding subgraphs. We now show how to create an `OptiGraph` using a *top-down* approach. Specifically, we show how to partition an `OptiGraph`, construct subgraphs from the partitions, and use these to derive an alternative representation of the `OptiGraph`. As part of this, we will discuss how `Plasmo.jl` interfaces to standard graph partitioning tools.

Function	Description
<code>OptiGraph()</code>	Create a new <code>OptiGraph</code> object.
<code>@optinode</code> (<code>graph::OptiGraph, expr::Expr</code>)	Create <code>OptiNodes</code> using <code>Julia</code> expression
<code>@linkconstraint</code> (<code>graph::OptiGraph, expr::Expr</code>)	Create linking constraint between nodes in <code>graph</code> using <code>expr</code>
<code>add_subgraph!</code> (<code>graph::OptiGraph, sg::OptiGraph</code>)	Add subgraph <code>sg</code> to <code>graph</code>
<code>getoptinodes</code> (<code>graph::OptiGraph</code>)	Retrieve local <code>OptiNodes</code> in <code>graph</code>
<code>getoptiedges</code> (<code>graph::OptiGraph</code>)	Retrieve local <code>OptiEdges</code> in <code>graph</code>
<code>getlinkconstraints</code> (<code>graph::OptiGraph</code>)	Retrieve linking constraints in <code>graph</code>
<code>getsubgraphs</code> (<code>graph::OptiGraph</code>)	Retrieve subgraphs in <code>graph</code>
<code>all_optinodes</code> (<code>graph::OptiGraph</code>)	Retrieve all <code>OptiNodes</code> in <code>graph</code> (including subgraphs)
<code>all_optiedges</code> (<code>graph::OptiGraph</code>)	Retrieve <code>OptiEdges</code> in <code>graph</code> (including subgraphs)
<code>all_linkconstraints</code> (<code>graph::OptiGraph</code>)	Retrieve all linking constraints in <code>graph</code> (including subgraphs)
<code>all_subgraphs</code> (<code>graph::OptiGraph</code>)	Retrieve all subgraphs in <code>graph</code> (including subgraphs)

Table 1: Overview of `OptiGraph` construction and query functions in `Plasmo.jl`.

2.4.1 Hypergraph Partitioning

The `OptiGraph` is, by default, a hypergraph; as such, we can naturally exploit hypergraph partitioning capabilities. Here, we focus on hypergraph partitioning concepts but we note that our discussion also applies to standard graph partitioning frameworks (a hypergraph can be projected to various standard graph representations). Hypergraph partitioning has received significant interest in the last few years because it naturally represents complex *non-pairwise* relationships and more accurately captures coupling in such structures compared to traditional graphs. Popular hypergraph partitioning tools include the well-known `hMetis` and `PaToH` packages, as well as the comprehensive `Zoltan` [17] software suite which provides hypergraph partitioning algorithms for `C`, `C++`, and `Fortran` applications. More recent frameworks have made advances to create large-scale hypergraphs [40], perform fast hypergraph partitioning [54], and create high-quality hypergraph partitions [66].

To provide an overview of hypergraph partitioning techniques, we use notation that is similar to that of an `OptiGraph`. A hypergraph contains a set of hypernodes $\mathcal{N}(\mathcal{H})$ and hyperedges $\mathcal{E}(\mathcal{H})$ where we denote the hypergraph containing hypernodes and hyperedges as $\mathcal{H}(\mathcal{N}, \mathcal{E})$. In hypergraph partitioning, one seeks to partition the set of nodes $\mathcal{N}(\mathcal{H})$ into a collection \mathcal{P} of at most k disjoint subsets such that $\mathcal{P} = \{P_1, P_2, \dots, P_k\}$ while minimizing an objective function over the edges such as (2.6a) or (2.6b) subject to a balance constraint (2.6c) (such that partitions are roughly the same size).

$$\Phi_{cut}(\mathcal{P}) = \sum_{e \in \mathcal{E}_{cut}(\mathcal{P})} w(e) \quad (2.6a)$$

$$\Phi_{con}(\mathcal{P}) = \sum_{e \in \mathcal{E}_{cut}(\mathcal{P})} w(e)(\lambda(e) - 1) \quad (2.6b)$$

$$\frac{1}{k} \sum_{n \in \mathcal{N}(\mathcal{H})} s(n) - \epsilon_{max} \leq \sum_{n \in P_i} s(n) \leq \frac{1}{k} \sum_{n \in \mathcal{N}(\mathcal{H})} s(n) + \epsilon_{max}, \quad \forall i \in \{1, \dots, k\} \quad (2.6c)$$

Here, Φ_{cut} and Φ_{con} are the most prominent hypergraph partitioning objectives (called the minimum edge-cut and minimum connectivity), where $\mathcal{E}_{cut}(\mathcal{P})$ is the set of *cut edges* of the partitions in \mathcal{P} (i.e., all edges that *cross* partitions defined by \mathcal{P}). The formulation in (2.6) introduces edge weights $w(e) \rightarrow \mathbb{R}$ for each edge $e \in \mathcal{E}(\mathcal{H})$ and node sizes $s(n) \rightarrow \mathbb{R}$ for each node $n \in \mathcal{N}(\mathcal{H})$ which can be used to express specific attributes to the partitioner. For instance, large edge weights

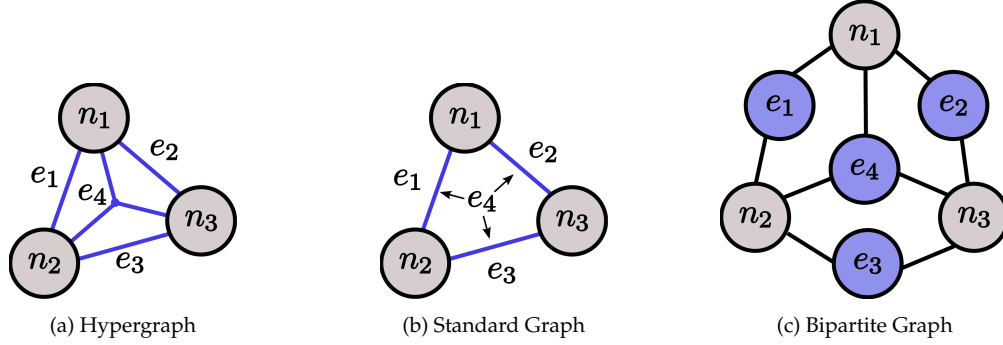


Fig. 10: Typical graph representations used in partitioning tools. A hypergraph can be projected to a standard graph or a bipartite graph.

typically express tight coupling or high communication volume and nodes sizes often represent computational load. The objective (2.6b) includes the connectivity value $\lambda(e)$ which denotes the number of partitions connected by a hyperedge e . We also define the parameter $\epsilon_{max} > 0$ in (2.6c) which specifies the maximum imbalance tolerance of the partitions. Lower values of ϵ_{max} enforce equal-sized partitions and higher values allow for solutions with disparate partition sizes. The lower bound constraint in (2.6c) is not always included in partitioning algorithm implementations.

The hypergraph is an intuitive representation for an `OptiGraph` but other representations are also possible. The hypergraph in Figure 10a can be projected to a standard graph representation (shown in Figure 10b) or to a bipartite representation (shown in Figure 10c). Standard graph representations of optimization problems can utilize mature partitioning tools such as `Metis` or community detection strategies. This provides flexibility to experiment with different techniques. In the remainder of the discussion we utilize the hypergraph representation for partitioning but we highlight that a broader range of partitioning strategies can be captured in the proposed framework.

2.4.2 `OptiGraph` Partitioning in `Plasmo.jl`

Here we discuss partitioning capabilities implemented in `Plasmo.jl`. Figure 11 depicts the basic aspects of the partitioning framework. We show how to create `OptiGraph` partitions (with a `Partition` object), how to formulate subgraphs (with the `make_subgraphs!` function), and how to *combine* (aggregate) subgraphs into stand-alone `OptiNodes` (with the `aggregate` function). For example, Figure 11a contains three partitions P_1, P_2 , and P_3 , Figure 11b shows the corresponding subgraphs $\mathcal{SG}_1, \mathcal{SG}_2$, and \mathcal{SG}_3 created from the partitions, and Figure 11c depicts the resulting `OptiNodes` n'_1, n'_2 , and n'_3 which represent optimization *subproblems*. To perform hypergraph partitioning we use the `KaHyPar` [66] hypergraph partitioner through the `KaHyPar.jl` interface. `KaHyPar` targets the creation of high quality partitions and offers a straightforward C library interface which facilitates its connection with `Plasmo.jl`. Throughout our examples we use the default `KaHyPar` configuration which uses a direct multilevel k-way algorithm with community detection initialization.

The `OptiGraph` object offers topology manipulation functionality that can be used, for instance, to modify subgraph structures and formulate subproblems for algorithms. Figure 12 de-

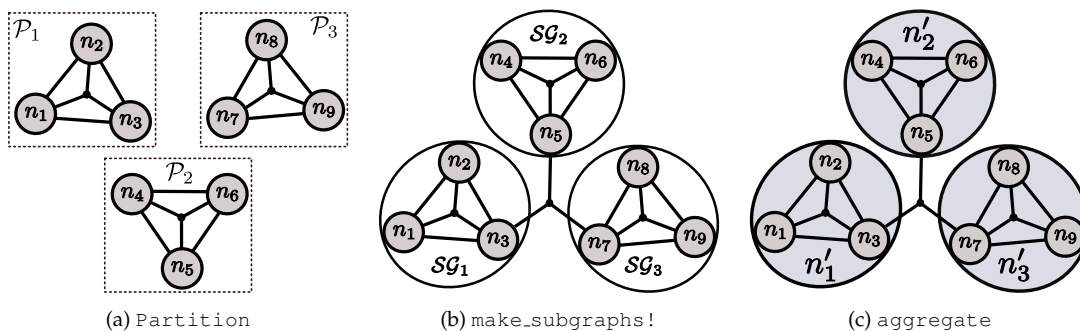


Fig. 11: Core partitioning functionality in `PlasmO.jl`. (left) A `Partition` with nine `OptiNodes`, (middle) corresponding `OptiGraph` containing three subgraphs, and (right) subgraphs aggregated into `OptiNodes`.

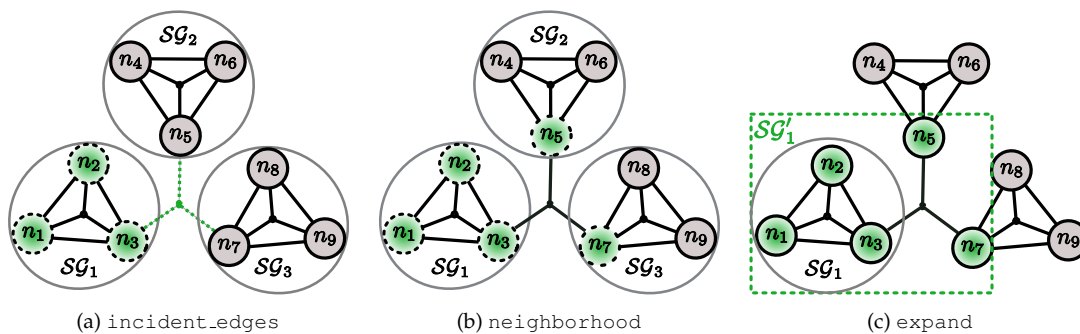


Fig. 12: Core graph topology functions in `PlasmO.jl`. (left) querying incident edges to a subgraph, (middle) querying a subgraph neighborhood, and (right) expanding a subgraph.

picts core topology functions we commonly use in the framework. We can query the incident `OptiEdges` (Figure 12a) to a set of `OptiNodes` (or a subgraph) to inspect coupling (i.e. inspect incident linking constraints). We can also obtain the neighborhood (Figure 12b) around a set of `OptiNodes` to inspect an expanded problem domain, and we can `expand` (Figure 12c) a subgraph into a larger domain and generate the corresponding subproblem.

Table 2 summarizes the core graph partitioning and manipulation functions in `PlasmO.jl`. The `gethypergraph` function returns a hypergraph object (extends a `LightGraphs.jl` object) and a `reference_map` which maps the hypergraph elements back to the `OptiGraph` (i.e. hypergraph node indices are mapped back to `OptiNodes`). We also introduce a `Partition` object that describes how to formulate subgraphs within a graph. As we will show, the `Partition` object is an intermediate interface to formulate subgraphs in a general way.

2.4.3 Example 4: Partitioning a Dynamic Optimization Problem

To demonstrate partitioning and manipulation capabilities, we use the simple dynamic optimization problem [73]:

Functions and Descriptions
Create a hypergraph representation of graph. <code>hypergraph, ref = gethypergraph(graph::OptiGraph)</code>
Create a Partition given an OptiGraph, a vector of integers and a mapping <code>ref_map</code> . <code>partition = Partition(graph::OptiGraph, vector::Vector{Int}, mapping::Dict{Int, OptiNode})</code>
Reform graph into subgraphs using partition. <code>make_subgraphs!(graph::OptiGraph, partition::Partition)</code>
Combine subgraphs in graph such that <code>n_levels</code> of subgraphs remain. <code>aggregate(graph::OptiGraph, n_levels::Int)</code>
Retrieve incident OptiEdges of OptiNodes in graph. <code>incident_optiedges(graph::OptiGraph, nodes::Vector{OptiNode})</code>
Retrieve neighborhood within distance of nodes. <code>neighborhood(graph::OptiGraph, nodes::Vector{OptiNode}, distance::Int)</code>
Retrieve a subgraph from graph including neighborhood nodes within distance of <code>sg</code> . <code>expand(graph::OptiGraph, sg::OptiGraph, distance::Int)</code>

Table 2: Overview of core partitioning and topology functions in `Plasmo.jl`.

$$\min_{\{x,u\}} \sum_{t=1}^T x_t^2 + u_t^2 \quad (2.7a)$$

$$\text{s.t. } x_{t+1} = x_t + u_t + d_t, \quad t \in \{1, \dots, T-1\} \quad (2.7b)$$

$$x_1 = 0 \quad (2.7c)$$

$$x_t \geq 0, \quad t \in \{1, \dots, T\} \quad (2.7d)$$

$$u_t \geq -1000, \quad t \in \{1, \dots, T-1\} \quad (2.7e)$$

Here, x is a vector of states and u is a vector of control actions which are both indexed over the set of time indices $t \in \{1, \dots, T\}$. Equation (2.7a) minimizes the state trajectory with minimal control effort (energy), (2.7b) describes the state dynamics, and (2.7c) is the initial condition. This problem can be formulated using an `OptiGraph` as shown in Code Snippet 4 in much the same way as the examples in Section 2.3. We define the number of time periods $T = 100$ and create a disturbance vector `d` (data) on Lines 1 through 6. In our implementation we create separate sets of nodes for the states and controls on Lines 12 and 13, but it is also possible to define nodes for each individual time interval and add state and control variables to the resulting nodes. Having control over this granularity is convenient for expressing what can be partitioned (i.e. features defined in an `OptiNode` will remain in the same partition). Next we setup the state and control `OptiNodes` on Lines 16 through 31, we use a linking constraint to capture dynamic coupling on Line 34 and we show how to solve the problem with `Ipopt` [79] on Line 39. We visualize the graph topology and matrix in Figure 13. The layouts depict a linear graph but we note that the matrix has no obvious structure.

We partition the graph using `KaHyPar`, as shown in Code Snippet 5; here, Line 2 imports the `KaHyPar` interface and Line 5 creates the hypergraph representation corresponding to the `OptiGraph` using `gethypergraph`. We also return a `reference_map` which maps the hypergraph elements back to the `OptiGraph`. Line 8 performs hypergraph partitioning using `KaHyPar` with a maximum imbalance (ϵ_{max}) of 10% and Line 11 creates a `Partition` object using the resulting partition vector and the `reference_map`. Line 14 creates subgraphs in the graph `graph` using the `Partition` object and the `make_subgraphs!` function. We visualize the topology and matrix of the partitioned problem on Lines 16 and 19 and these are shown in Figure 14. This reveals eight distinct partitions and their corresponding coupling. We note that the partitions are

Code Snippet 4: Construction of dynamic optimization problem (2.7)

```

1  using Plasmo
2  using Plots
3  using Ipopt
4
5  T = 100 #number of time points
6  d = sin.(1:T) #disturbance
7
8  #Create an OptiGraph
9  graph = OptiGraph()
10
11 #Add nodes for states and controls
12 @optinode(graph, state[1:T])
13 @optinode(graph, control[1:T-1])
14
15 #Add state variables
16 for (i,node) in enumerate(state)
17     @variable(node,x)
18     @constraint(node, x >= 0)
19     @objective(node,Min,x^2)
20 end
21
22 #Add control variables
23 for node in control
24     @variable(node,u)
25     @constraint(node, u >= -1000)
26     @objective(node,Min,u^2)
27 end
28
29 #Initial condition
30 n1 = state[1]
31 @constraint(n1,n1[:x] == 0)
32
33 #Dynamic coupling
34 @linkconstraint(graph,[t = 1:T-1],state[t+1][:x] == state[t][:x] +
35                 control[t][:u] + d[t])
36
37 #Optimize with Ipopt
38 ipopt = Ipopt.Optimizer
39 optimize!(graph,ipopt)
40
41 #Plot result structure
42 plt_graph4 = plot(graph,
43                 layout_options = Dict(:tol => 0.1,:iterations => 500),
44                 linealpha = 0.2,markersize = 6)
45
46 plt_matrix4 = spy(graph)

```

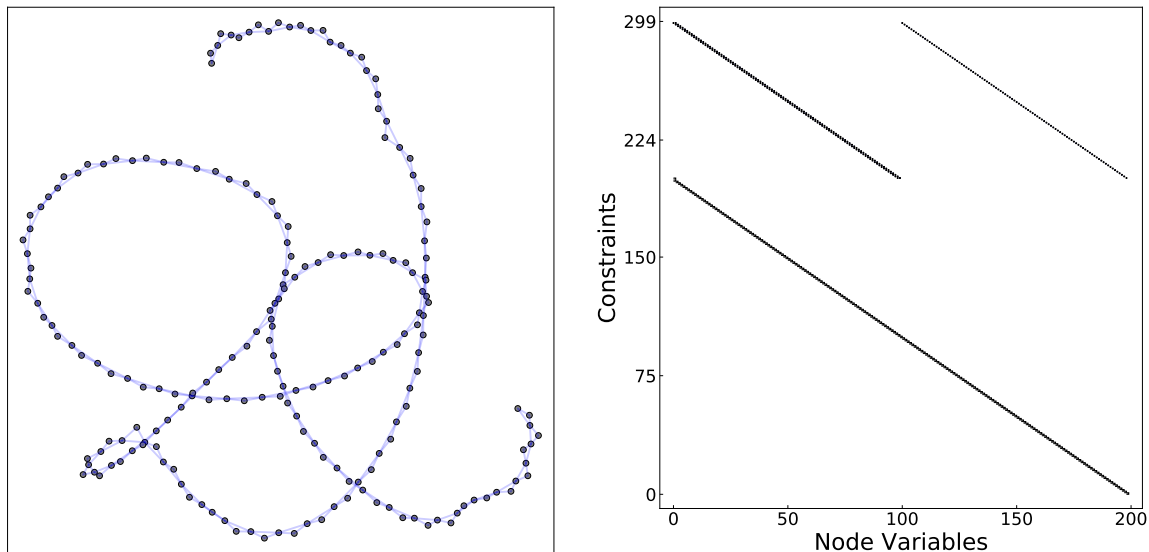


Fig. 13: Output visuals for Code Snippet 4 showing graph structure of dynamic optimization problem.

Code Snippet 5: Creating subgraphs using hypergraph partitioning with KaHyPar

```

1 #Import KaHyPar interface
2 using KaHyPar
3
4 #Create a hypergraph representation of the OptiGraph
5 hypergraph,reference_map = gethypergraph(graph)
6
7 #Perform hypergraph partitioning using KaHyPar
8 node_vector = KaHyPar.partition(hypergraph,8,imbalance = 0.1)
9
10 #Create a Partition object
11 partition = Partition(graph,node_vector,reference_map)
12
13 #Create subgraphs using the partition object and reference_map
14 make_subgraphs!(graph,partition)
15
16 plt_graph5 = plot(graph,
17 layout_options = Dict(:tol => 0.01,:iterations => 500),
18 linealpha = 0.2,markersize = 6,subgraph_colors = true);
19 plt_matrix5 = spy(graph,subgraph_colors = true);

```

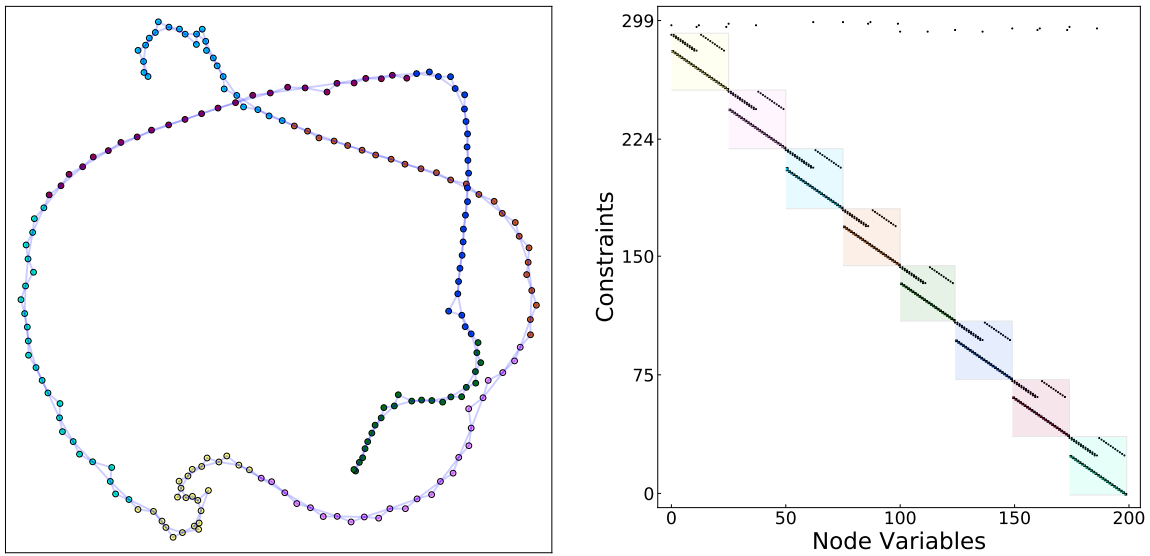


Fig. 14: Output visuals for Code Snippet 5 showing partitions and reordering of dynamic optimization problem.

well-balanced and note that the matrix is now rearranged into a banded structure that is typical of dynamic optimization problems (partitioning automatically induces reordering). `Plasmo.jl` can use other graph representations to perform partitioning. For instance, we can create a traditional graph representation, as shown in Code Snippet 6, and partition it with `Metis`. We then use the `reference_map` to obtain the original `OptiGraph` elements to create a graph `Partition`. We could also partition less intuitive representations (e.g., bipartite) in this way; we only require a mapping from the partition back to the `OptiGraph` elements. The partitioning procedure shown here can also be repeated to create an arbitrary number of subgraph levels.

The `OptiNodes` in a graph can be *aggregated* to form larger nodes, as shown in Figure 11c. This aggregation functionality is key to communicate subproblems to decomposition algorithms that

Code Snippet 6: Creating a subgraph partition using graph partitioning with `Metis`

```

1 #Import the Metis interface
2 using Metis
3
4 #Retrieve underlying hypergraph from dynamic opt problem graph
5 simple_graph, reference_map = getcliquegraph(graph)
6
7 #Run Metis direct k-way partitioning with a 8 maximum of partitions
8 node_vector = Metis.partition(simple_graph, 8, alg = :KWAY)
9
10 #Create a Partition object using node vector and reference_map
11 partition = Partition(graph, node_vector, reference_map)
12
13 #Create subgraphs using Partition object
14 make_subgraphs!(graph, partition)

```

operate at different levels of granularity. Aggregation can also be performed to collapse an entire graph into a single node, producing a standard optimization problem that can be solved with off-the-shelf solvers. Code Snippet 7 shows how to aggregate the graph of the dynamic optimization problem into a new aggregated graph with eight nodes. We create the new (`aggregated_graph`) on Line 2 by using `aggregate` on the `graph` from Snippet 5. We provide the integer 0 to the function to specify that we want zero subgraph levels which converts the eight subgraphs into nodes. For hierarchical graphs with many levels, we can define how many subgraph levels we wish to retain. We plot the graph and matrix layouts for the aggregated `OptiGraph` on Lines 5 and 8 and these are shown in Figure 15.

2.4.4 Example 5: Using Graph Topology Functions

We now show how to use graph topology functions by computing *overlapping* partitions for the dynamic optimization example. This is shown in Code Snippet 8; here, Line 2 obtains subgraphs from the `OptiGraph` `graph` created in Snippet 5, Line 8 determines and returns the `OptiEdges` incident to the `OptiNodes` in the first subgraph `sg1`, and Line 12 returns the complete neighborhood around the same `OptiNodes` within a distance of two. On Line 16, we broadcast the `expand` function (using dot syntax `expand.()` and `Ref` as typical in Julia) to create a new set of subgraphs, each expanded by a distance of two. Line 19 plots the layout of `graph` with the expanded subgraphs as is shown in Figure 16. Here, we see eight distinct partitions (each with a unique color) where the larger markers represent nodes that are part of multiple subgraphs (they are also the average color of their containing subgraphs). Figure 16 shows the corresponding matrix layout where highlighted columns indicate that the node also appears in other subgraph blocks. Overlapping partitions are useful in certain algorithms such as Schwarz decomposition.

Code Snippet 7: Aggregating nodes in an OptiGraph

```

1 #Combine the subgraphs in graph into OptiNodes in a new OptiGraph
2 aggregated_graph,ref_map = aggregate(graph,0)
3
4 #plot the graph a matrix layouts of the aggregated OptiGraph
5 plt_graph6 = plot(aggregated_graph,
6 layout_options = Dict(:tol => 0.01,:iterations => 10),
7 node_labels = true,markersize = 30,labelsiz = 20,node_colors = true)
8 plt_matrix6 = spy(aggregated_graph,node_labels = true,node_colors = true)

```

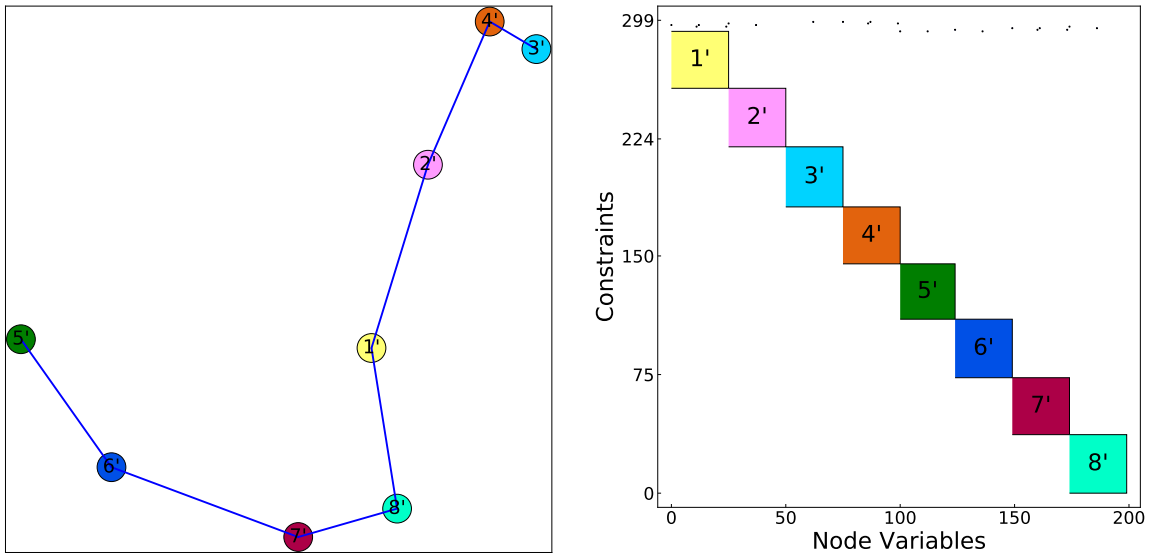


Fig. 15: Output visuals for Code Snippet 7 showing aggregated graph of dynamic optimization problem.

Code Snippet 8: Using Graph Topology Functions

```

1 #Get the current subgraphs in graph
2 subgraphs = getsubgraphs(graph)
3
4 #Query the first subgraph
5 sg1 = subgraphs[1]
6
7 #Query the edges incident to the nodes in sg1
8 incident_edges = incident_edges(graph,all_nodes(sg1))
9
10 distance = 2
11 #Query the nodes within distance 2 of sg1
12 nodes = neighborhood(graph,all_nodes(sg1),distance)
13
14 #Broadcast expand function to each subgraph.
15 #Obtain vector of expanded subgraphs
16 expanded_subgraphs = expand.(Ref(graph), subgraphs,Ref(distance))
17
18 #Plot the expanded subgraphs
19 plt_graph7 = plot(graph,expanded_subgraphs,
20 layout_options = Dict(:tol => 0.01,:iterations => 1000),
21 markersize = 6,linealpha = 0.2)
22 plt_matrix7 = spy(graph,expanded_subgraphs)

```

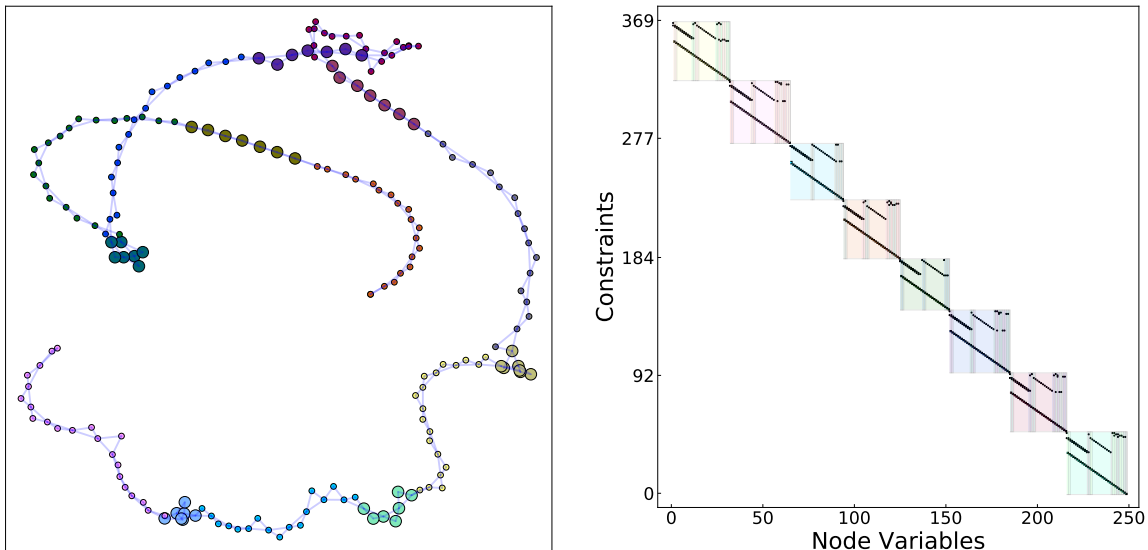


Fig. 16: Output visuals for Code Snippet 8 showing overlapping subgraphs.

3 Algorithms

The `OptiGraph` provides a flexible abstraction that facilitates communication of problem structure to a wide range of decomposition strategies. The structure can be exploited at a problem level, in which the decomposition strategy treats `OptiNodes` as optimization subproblems whose solutions are coordinated to find a solution of the entire `OptiGraph`. This strategy is used, for example, in Benders, Lagrangian dual, and ADMM decomposition. The structure can also be exploited at the linear algebra level, in which a decomposition strategy is used within a general algorithm to compute a search step. Here, the strategy treats `OptiNodes` as linear systems that result from the optimality conditions of the associated subproblems and coordinates their solutions to find a solution of the linear system associated with the optimality conditions of the entire `OptiGraph`. In this section we show how to use the proposed abstraction and `Plasmo.jl` functionality to explain structures at the linear algebra and problem level.

3.1 Linear Algebra Decomposition

It is well-known that block structures can be exploited by linear algebra operations within interior-point algorithms. For instance, continuous problems with the partially-separable structure described by (2.1) induce structured linear algebra kernels that can be solved using tailored techniques such as Schur decomposition. We express the continuous variant of the graph formulation (2.1) with feasible sets of the form $\mathcal{X}_n := \{x \mid c_n(x) = 0\}$ which gives rise to the Karush-Kuhn-Tucker (KKT) system given by:

$$\sum_{n \in \mathcal{N}(\mathcal{G})} \left(\nabla_{x_n} f_n(x_n) + \nabla_{x_n} c_n(x_n) \lambda_n \right) + \sum_{e \in \mathcal{E}(\mathcal{G})} \nabla_{\{x_n\}_{n \in \mathcal{N}(e)}} g_e(\{x_n\}_{n \in \mathcal{N}(e)}) \lambda_e = 0, \quad (3.8a)$$

$$c_n(x_n) = 0, \quad n \in \mathcal{N}(\mathcal{G}), \quad (3.8b)$$

$$g_e(\{x_n\}_{n \in \mathcal{N}(e)}) = 0, \quad e \in \mathcal{E}(\mathcal{G}). \quad (3.8c)$$

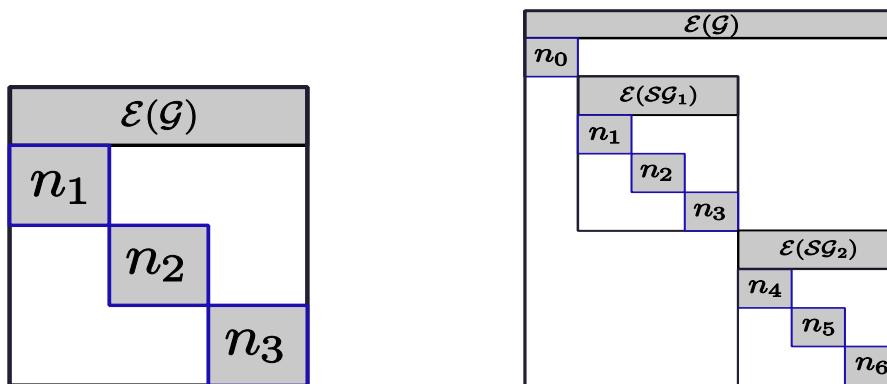


Fig. 17: Block structure (left) and nested block structure (right) of an `OptiGraph`.

Here, we recall that $\mathcal{N}(e)$ denotes the nodes that support edge e . The terms associated with barrier functions exist in (3.8) in the presence of inequality constraints. Upon linearization of (3.8), the system of algebraic equations gives rise to the block-bordered KKT system given by:

$$\left[\begin{array}{ccc|c} K_{n_1} & & & B_{n_1} \\ & K_{n_2} & & B_{n_2} \\ & & \ddots & \vdots \\ & & & K_{n_{|\mathcal{N}|}} & B_{n_{|\mathcal{N}|}} \\ \hline B_{n_1}^T & B_{n_2}^T & \cdots & B_{n_{|\mathcal{N}|}}^T & \end{array} \right] \begin{bmatrix} \Delta w_{n_1} \\ \Delta w_{n_2} \\ \vdots \\ \Delta w_{n_{|\mathcal{N}|}} \\ \Delta \lambda_{\mathcal{E}(\mathcal{G})} \end{bmatrix} = - \begin{bmatrix} r_{n_1} \\ r_{n_2} \\ \vdots \\ r_{n_{|\mathcal{N}|}} \\ r_{\mathcal{E}(\mathcal{G})} \end{bmatrix}. \quad (3.9)$$

Here, $\Delta w_n := (\Delta x_n, \Delta \lambda_n)$ is the primal-dual step for the variables and constraints on node n and $\Delta \lambda_{\mathcal{E}(\mathcal{G})}$ is a vector of steps corresponding to the dual variables on the `OptiEdges` in `OptiGraph` \mathcal{G} , where $\Delta \lambda_{\mathcal{E}(\mathcal{G})} := \{\Delta \lambda_e\}_{e \in \mathcal{E}(\mathcal{G})}$. We also define

$$K_n := \begin{bmatrix} W_n & J_n^T \\ J_n & 0 \end{bmatrix},$$

as the block matrix corresponding to `OptiNode` n where $W_n = \nabla_{x_n, x_n} \mathcal{L}$ is the Hessian of the Lagrange function of (2.1) and $J_n := \nabla_{x_n} c_n(x_n)$ is the constraint Jacobian. We define coupling blocks B_n as

$$B_n := \begin{bmatrix} Q_n & 0 \\ 0 & 0 \end{bmatrix},$$

where $Q_n := \nabla_{x_n} \{g_e(\{x_{n'}\}_{n' \in \mathcal{E}(n)})\}_{e \in \mathcal{E}(\mathcal{G})}$. If all of the linking constraints in the graph are *linear*, Q_n reduces to Π_n^T where Π_n is the matrix of coefficients corresponding to the `OptiEdges` incident to node n .

3.1.1 Schur Decomposition

The block-bordered structure described in (3.8) can be exploited using Schur decomposition or block preconditioning strategies. The typical Schur decomposition algorithm is described by (3.10) in terms of the `OptiGraph` abstraction, where S is the Schur complement matrix.

$$S = - \sum_{n \in \mathcal{N}(\mathcal{G})} B_n^T K_n^{-1} B_n \quad (3.10a)$$

$$S \Delta \lambda_{\mathcal{E}(\mathcal{G})} = \sum_{n \in \mathcal{N}(\mathcal{G})} B_n^T K_n^{-1} r_n - r_{\mathcal{E}(\mathcal{G})} \quad (3.10b)$$

$$K_n \Delta w_n = B_n \Delta \lambda_{\mathcal{E}(\mathcal{G})} - r_n \quad (3.10c)$$

Step (3.10a) requires factorizing the linear system associated to each `OptiNode` (K_n) and computes the Schur complement contribution $B_n^T K_n^{-1} B_n$ on each node (possibly in parallel). After each contribution is computed (each requires performing a sparse factorization), the total Schur complement matrix S is created and factorized to solve the linear system (3.10b) (in serial) and take a step in the `OptiEdge` dual variables ($\lambda_{\mathcal{E}(\mathcal{G})}$). Step (3.10c) solves for the `OptiNode` primal-dual step Δw_n given the `OptiEdge` dual step (also possibly in parallel).

The general Schur decomposition exhibits a couple of major *computational bottlenecks*. Forming the contributions $B_n^T K_n^{-1} B_n$ is expensive when there are many columns in B_n (the number of columns corresponds to the number linking constraints incident to node n). Moreover, if the node blocks have different sizes, the factorization of the blocks K_n can create load imbalance and memory issues. Second, factorizing the Schur matrix S is challenging when there are many linking constraints because this matrix is dense or is composed of dense sub-blocks. Consequently, one needs to control the amount of coupling between the blocks. The `OptiGraph` topology directly corresponds with the size of the block matrices that appear in the Schur decomposition and thus can be manipulated to facilitate computational efficiency. Specifically, we wish to manipulate the partitioning of an `OptiGraph` to accelerate Schur decomposition. We use the capabilities of `Plasmo.jl` to experiment with different partitioning strategies and with this analyze trade-offs between coupling, imbalance, and memory use. Section 4.1 details these performance trade-offs with a large example.

3.1.2 PIPS-NLP Interface

`Plasmo.jl` includes an interface to the structure-exploiting interior-point solver PIPS-NLP that we call

`PipsSolver.jl`. PIPS-NLP provides a general Schur decomposition strategy that performs parallel computations via MPI. PIPS-NLP was developed to solve large-scale stochastic programming problems that adhere to a two-level tree structure (i.e. a single first stage problem coupled to second stage subproblems). The `OptiGraph` interface to PIPS-NLP converts general graph structures into this format (e.g., via aggregation and partitioning). For instance, using our example problem (2.7), we can communicate the problem structure to PIPS-NLP and solve the problem in parallel. This is shown in Snippet 9.

Code Snippet 9: Solving an `OptiGraph` model in parallel with PIPS-NLP

```

1  using Distributed
2  using MPIClusterManagers
3
4  # specify, number of mpi workers
5  manager=MPIManager(np=2)
6  # start mpi workers and add them as julia workers too.
7  addprocs(manager)
8
9  #Setup the worker environments
10 @everywhere using Plasmo
11 @everywhere using PipsSolver #Solver interface to PIPS-NLP
12
13 #get the julia ids of the mpi workers
14 julia_workers = collect(values(manager.mpi2j))
15
16 #Use the pips-nlp interface to distribute the OptiGraph among workers
17 #Here, we create the variable 'pips_graph' on each worker
18 remote_references = PipsSolver.distribute(graph, julia_workers,
19 remote_name = :pips_graph)
20
21 #Solve with PIPS-NLP
22 @mpi_do manager begin
23     using MPI
24     PipsSolver.pipsnlp_solve(pips_graph)
25 end

```

Snippet 9 presents a standard template for setting up distributed computing environments to use `PipsSolver.jl` which is worth discussing. Line 1 imports the `Distributed` module, which is a Julia package for performing distributed computing. On Line 2 we import the `MPIClusterManagers` package which allows us to interface MPI ranks (used by PIPS-NLP) with Julia worker CPUs.

We create a `manager` object and specify that we want to use 2 workers on Line 5 and add the Julia workers on Line 7. Next we setup the model and solver environments for the added workers on Lines 10 and 11 and create a reference to the Julia workers by querying the manager on Line 14. We *distribute* the graph among the workers in Line 18 using the function provided by `PipsSolver`. This function sets up the relevant graph nodes on each worker and creates the graph named `pips_graph` on each worker (internally this function inspects the `OptiGraph` and allocates `OptiNodes` to worker CPUs). Finally, we use the `mpi_do` function from `MPIClusterManagers` to execute MPI on each worker and solve the graph. Each worker executes the `pinlp_solve` function and communicates using MPI routines within `PIPS-NLP`.

3.2 Problem Level Decomposition

Overlapping Schwarz is a flexible graph-based decomposition strategy that can be used at the linear algebra or problem level [24,74]. This approach has been used to solve dynamic optimization [71] and network optimization problems [70]. At the problem level, the Schwarz algorithm decomposes the problem graph over *overlapping* partitions. The algorithm solves subproblems over the overlapping partitions and coordinates solutions by exchanging primal-dual information over the overlapping regions. The presence of overlap is key to promote convergence; in particular, it has been proven that the convergence rate improves exponentially with the size of the overlap [74]. The Schwarz scheme is also flexible in that the overlap can be adjusted to trade-off subproblem complexity (time and memory) with convergence speed. When the overlap is the entire graph, the algorithm solves the entire graph once (converges in one iteration). When the overlap is zero, the algorithm operates as a standard Gauss-Seidel scheme and will exhibit slow convergence (or no convergence at all). We thus have that Schwarz has fully centralized and fully decentralized schemes as extremes. Schwarz algorithms can also be implemented under synchronous and asynchronous settings to handle load imbalance issues [74].

3.2.1 Development of Schwarz Algorithm

The Schwarz algorithm iteratively solves subproblems associated with overlapping subgraphs. In particular, one first constructs *expanded subgraphs* $\{\mathcal{SG}'_i\}_{i=1}^N$ from the subgraphs $\{\mathcal{SG}_i\}_{i=1}^N$ obtained from `OptiGraph` partitioning. This procedure can be performed by expanding the subgraphs and adding `OptiNodes` within a prescribed distance $\omega \geq 0$. The optimization subproblems for the expanded subgraph \mathcal{SG}'_i can be formulated as:

$$\min_{\{x_n\}_{n \in \mathcal{N}(\mathcal{SG}'_i)}} \sum_{n \in \mathcal{N}(\mathcal{SG}'_i)} f_n(x_n) - \sum_{e \in \mathcal{I}_1(\mathcal{SG}'_i)} (\lambda_e^k)^T g_e(\{x_n\}_{n \in \mathcal{N}(e) \cap \mathcal{N}(\mathcal{SG}'_i)}, \{x_n^k\}_{n \in \mathcal{N}(e) \setminus \mathcal{N}(\mathcal{SG}'_i)}) \quad (3.11a)$$

$$\text{s.t. } x_n \in \mathcal{X}_n, \quad n \in \mathcal{N}(\mathcal{SG}'_i), \quad (3.11b)$$

$$g_e(\{x_n\}_{n \in \mathcal{N}(e)}) = 0, \quad e \in \mathcal{E}(\mathcal{SG}'_i), \quad (3.11c)$$

$$g_e(\{x_n\}_{n \in \mathcal{N}(e) \cap \mathcal{N}(\mathcal{SG}'_i)}, \{x_n^k\}_{n \in \mathcal{N}(e) \setminus \mathcal{N}(\mathcal{SG}'_i)}) = 0, \quad e \in \mathcal{I}_2(\mathcal{SG}'_i). \quad (3.11d)$$

Here, the dual variables for (3.11c) and (3.11d) are denoted by λ_e , $\mathcal{N}(\mathcal{SG}'_i)$ is the set of nodes in subgraph \mathcal{SG}'_i , and the superscript $(\cdot)^k$ denotes the iteration counter. For representation we denote \mathcal{I}_1 and \mathcal{I}_2 as two separate sets of incident edges where $\mathcal{I} := \mathcal{I}_1 \cup \mathcal{I}_2$. More specifically, $\mathcal{I}(\mathcal{SG}'_i)$ is

the set of edges incident to \mathcal{SG}'_i (i.e. edges that contain a node in another subgraph) and \mathcal{I}_1 and \mathcal{I}_2 denote how the incident linking constraints are formulated within the subproblem using either primal or dual coupling.

In our formulation, (3.11a) is the subproblem objective which is the sum of node objective functions contained in the expanded subgraph \mathcal{SG}'_i where we have added the dual penalties from the incident dual linking constraints on edges $e \in \mathcal{I}_1(\mathcal{SG}'_i)$, and (3.11d) represents primal constraints we have added from the edges $e \in \mathcal{I}_2(\mathcal{SG}'_i)$. Note that incident linking constraints can be directly incorporated into the subproblem as local constraints, or included in the objective function as a dual penalty (this assigning procedure can be important to the algorithm performance). In our implementation, one may provide preference on whether a linking constraint is treated in primal or dual form (we show in Section 4.2 how to do this). The primal-dual solution of the other subproblems obtained from the previous iteration, in particular $\{\{x_n^k\}_{n \in \mathcal{N}(e) \setminus \mathcal{N}(\mathcal{SG}'_i)}\}_{e \in \mathcal{I}(\mathcal{SG}'_i)}$ and $\{\lambda_e^k\}_{e \in \mathcal{I}_1(\mathcal{SG}'_i)}$, also enter into the subproblem formulation. The Schwarz algorithm achieves convergence with this exchange of information.

An important step in the Schwarz algorithm is the *restriction* of the subproblem solution. One obtains the primal-dual solution $\{x_n^*\}_{n \in \mathcal{N}(\mathcal{SG}'_i)}$ and $\{\{\lambda_e^*\}_{e \in \mathcal{E}(\mathcal{SG}'_i) \cup \mathcal{I}_2(\mathcal{SG}'_i)}\}$ by solving (3.11). We observe that the solutions from different subproblems overlap (the solution for overlapping nodes may appear more than once). We thus use a restriction step to eliminate such multiplicity; in particular, we discard the part of the solution associated with the nodes that are acquired by expansion. The restriction step can be expressed as:

$$\forall i \in \{1, 2, \dots, N\}, \quad \{x_n^k\}_{n \in \mathcal{N}(\mathcal{SG}_i)}, \{\lambda_e^k\}_{e \in \mathcal{E}(\mathcal{SG}_i)} \leftarrow \text{solution of (3.11)}.$$

The solution of subproblems $i = 1, 2, \dots, N$ can be performed in parallel. Next, the primal-dual residual at any Schwarz iteration k is evaluated according to the residual to the KKT system for (3.12). We define $r_e^{k,Pr}$ as the primal residual of the linking constraints on edge e at iteration k , and $r_e^{k,Du}$ as the dual residual of the linking constraints on edge e . Specifically, the primal error evaluates the linking constraints in the higher level graph $e \in \mathcal{E}(\mathcal{G})$, and the dual error evaluates the consensus of the dual values of the expanded subgraphs that contain the edge e ; for the case where more than two subgraphs are associated with one linking constraint, see [70, Proposition 1] for details on how to evaluate dual infeasibility. The formal definition of these residuals is given by:

$$r_e^{k,Pr} := g_e(\{x_n^k\}_{n \in \mathcal{N}(e)}), \quad e \in \mathcal{E}(\mathcal{G}), \quad (3.12a)$$

$$r_e^{k,Du} := \lambda_e^k(\mathcal{SG}'_i) - \lambda_e^k(\mathcal{SG}'_j), \quad e \in \mathcal{E}(\mathcal{G}). \quad (3.12b)$$

The termination criteria can be set as follows:

$$\text{stop if: } \max_{e \in \mathcal{E}(\mathcal{G})} \|r_e^{k,Pr}\|_\infty, \max_{e \in \mathcal{E}(\mathcal{G})} \|r_e^{k,Du}\|_\infty \leq \epsilon^{tol}, \quad (3.13)$$

where ϵ^{tol} is the prescribed convergence tolerance.

The Schwarz algorithm can be expressed using syntax that closely matches that of the OptiGraph abstraction, as shown in Algorithm 1. Figure 18 depicts how primal-dual information is exchanged in the overlapping subgraph scheme. The figure also depicts a simple graph that contains two subgraphs \mathcal{SG}_1 and \mathcal{SG}_2 and one edge e_2 that connects the subgraphs ($e_2 \in \mathcal{E}(\mathcal{G})$). The right side of Figure 18 shows the expanded subgraphs \mathcal{SG}'_1 and \mathcal{SG}'_2 . In this illustration, edge e_1 is incident to subgraph \mathcal{SG}'_2 and communicates primal information (i.e. it is in the set $\mathcal{I}_2(\mathcal{SG}'_2)$),

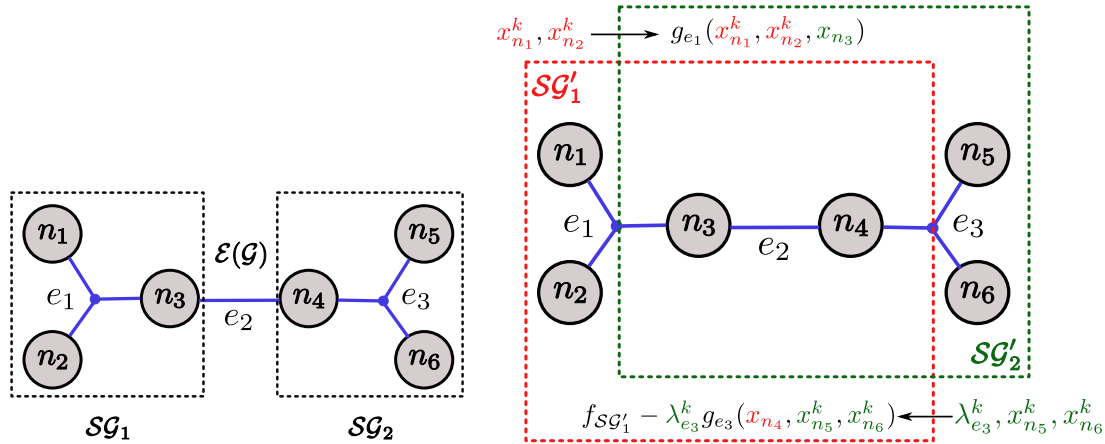


Fig. 18: Depiction of Schwarz Algorithm. The original graph containing two subgraphs (SG_1 and SG_2) connected by edge e_2 (left), graph with expanded subgraphs (SG'_1 and SG'_2) (right). The expanded subgraphs overlap at nodes n_3 and n_4 .

and edge e_3 is incident to subgraph SG'_1 and communicates dual information to subgraph SG'_1 (i.e. it is in the set $\mathcal{I}_1(SG'_1)$).

Algorithm 1 Schwarz Algorithm for Solving an OptiGraph

Input graph \mathcal{G} , non-expanded subgraphs $\{SG_1, \dots, SG_N\}$ and expanded subgraphs $\{SG'_1, \dots, SG'_N\}$.
Initialize x^0, λ^0
Formulate subproblems in (3.11)
while termination criteria not satisfied **do**
 for $i = 1 : N$ (in parallel) **do**
 Retrieve $\{\{x_n^k\}_{n \in \mathcal{N}(e) \setminus \mathcal{N}(SG'_i)}\}_{e \in \mathcal{I}(SG'_i)}$ and $\{\lambda_e^k\}_{e \in \mathcal{I}_1(SG'_i)}$ and update subproblems.
 Solve subproblem (3.11) to obtain $\{x_n^{k+1}\}_{n \in \mathcal{N}(SG_i)}$, $\{\lambda_e^{k+1}\}_{e \in \mathcal{E}(SG_i)}$
 end for
 Compute $\{r_e^{k,Pr}\}_{e \in \mathcal{E}(\mathcal{G})}$, $\{r_e^{k,Du}\}_{e \in \mathcal{E}(\mathcal{G})}$ and evaluate termination criteria (3.13).
end while

3.2.2 Implementation of Schwarz Algorithm

We implemented the Schwarz algorithm in `Plasmo.jl` and call this `SchwarzSolver.jl`. Code Snippet 10 shows how we can solve the overlapping subgraphs we produced in Code Snippet 8 corresponding to the overlap shown in Figure 16. On Line 1 we import the Schwarz solver, on Line 5 we create an `Ipopt` optimizer to use as the subproblem solver, and we execute the algorithm on Line 8. It is also possible to pass an overlap distance instead of the expanded subgraphs and allow the Schwarz solver to perform the subgraph expansion. The benefit of formulating subgraphs at the user level is that one could formulate custom overlap schemes.

Code Snippet 10: Using the Schwarz.jl Solver

```

1 using SchwarzSolver
2 using Ipopt
3
4 #Use Ipopt as the subproblem solver
5 ipopt = Ipopt.Optimizer
6
7 #Solve with Schwarz Algorithm
8 schwarz_solve(graph, expanded_subgraphs,
9 sub_optimizer = ipopt, max_iterations = 100, tolerance = 1e-6)

```

4 Case Studies

We demonstrate modeling and solution capabilities enabled by the `OptiGraph` abstraction and the `Plasmo.jl` implementation using a couple of challenging problems arising in infrastructure networks. The implementations used for the case studies can be found at <https://github.com/zavalab/JuliaBox/tree/master/PlasmoExamples>. We highlight that the study presented in Section 4.1 uses a dataset that cannot be shared (we only present computational results to demonstrate scalability). In the GitHub repository we provide a simple network dataset that uses the same features of `Plasmo.jl`.

4.1 Linear Algebra Decomposition of a Natural Gas Network

We solve a large dynamic optimization problem for the natural gas network shown in Figure 1a. This network includes four gas supplies, 153 time-varying gas demands, 215 pipelines, and 16 compressor stations. The goal of the optimization problem is to track demands and minimize compressor power over a 24-hour time horizon. The main complexity of this problem arises from nonlinear PDEs needed to capture conservation of mass and momentum inside the pipelines. After space-time discretization of the PDE, we obtain a nonconvex NLP with 432,048 variables, 427,512 equality constraints, and 3,887 inequality constraints. Figure 2b depicts the graph structure induced by the space-time nature of this problem. Our goal is to identify efficient partitions that traverse space-time to efficiently solve the problem using Schur decomposition in PIPS-NLP.

All model details can be found in [82] and [39] and in the scripts provided with this work. Here we provide a summary to showcase modeling features of `Plasmo.jl`. The gas network contains links and junctions $Net(\mathcal{J}, \mathcal{L})$. The set of junctions $j \in \mathcal{J}$ connect links and include gas supplies (injections) \mathcal{S}_j and demands (withdrawals) \mathcal{D}_j . The set of links \mathcal{L} is composed of both pipeline links \mathcal{L}_p and compressor links \mathcal{L}_c such that $\mathcal{L} := \mathcal{L}_p \cup \mathcal{L}_c$. We also specify the set of time periods as $\mathcal{T} := \{1, \dots, N_t\}$ with a 24-hour horizon and $\overline{\mathcal{T}} := \mathcal{T} \setminus N_t$. For our implementation, each component of the system is modeled as a stand-alone `OptiGraph` with `OptiNodes` distributed over time and we connect these in a high-level graph to form the complete problem. This modular construction is one of the benefits of the graph abstraction. Specifically, component models can be developed separately (e.g., by different people). Moreover, the syntax of the different components can be different because each `OptiGraph` is a self-contained object. This greatly facilitates model construction and debugging. This differs from standard algebraic modeling languages, in which the syntax in the entire model has to be compatible (this complicates debugging of large models). The implementations to construct each component model (each `OptiGraph`) in `Plasmo.jl` can be found in the Appendix.

Junction OptiGraph

The gas junction model is described by (4.14), where $\theta_{j,t}$ is the pressure at junction j and time interval t . $\underline{\theta}_j$ is the lower pressure bound for the junction, $\bar{\theta}_j$ is the upper pressure bound, $f_{j,d,t}^{target}$ is the target demand flow for demand d on junction j and $\bar{f}_{j,s}$ is the available gas generation from supply s on junction j . Code Snippet 13 in the Appendix shows how to create the junction graph.

$$\underline{\theta}_n \leq \theta_{j,t} \leq \bar{\theta}_n, \quad j \in \mathcal{J}, t \in \mathcal{T} \quad (4.14a)$$

$$0 \leq f_{j,d,t} \leq f_{j,d,t}^{target}, \quad d \in \mathcal{D}_j, j \in \mathcal{J}, t \in \mathcal{T} \quad (4.14b)$$

$$0 \leq f_{j,s,t} \leq \bar{f}_{j,s}, \quad s \in \mathcal{S}_j, j \in \mathcal{J}, t \in \mathcal{T}. \quad (4.14c)$$

Pipeline OptiGraph

Each pipeline model is an OptiGraph with OptiNodes distributed on a space-time grid. Specifically, the nodes of each pipeline graph form a $N_t \times N_x$ mesh wherein pressure and flow variables are assigned to each node. Flow dynamics within pipelines are expressed with linking constraints that describe the discretized PDE equations for mass and momentum using finite differences. We assume isothermal flow through each horizontal pipeline segment $\ell \in \mathcal{L}_p$ which are described by the conservation equations from [57]. The pipeline formulation is given by (4.15) where $p_{\ell,t,k}$ and $f_{\ell,t,k}$ are the pipeline pressure and flow for each pipeline link ℓ at each time period $t \in \mathcal{T}$ for each space point $k \in \mathcal{X}$ where $\mathcal{X} := \{1, \dots, N_x\}$ is the set of spatial discretization points we use for each pipeline. We also define $\bar{\mathcal{X}} := \mathcal{X} \setminus N_x$ for convenience. The constants given in this formulation for each pipeline $\ell \in \mathcal{L}_p$ are $c_{1,\ell} = \alpha \frac{c^2}{A_\ell}$, $c_{2,\ell} = \frac{1}{\alpha} A_\ell$, and $c_{3,\ell} = \alpha \frac{8c^2 \lambda_\ell A_\ell}{\pi^2 D_\ell^5}$. Here, the pipeline terms are the cross-sectional area A_ℓ , diameter D_ℓ , friction coefficient λ_ℓ , the gas speed of sound squared c^2 , and the scaling coefficient α . We denote expressions for the flow in and out of each pipeline at each time as $f_{\ell,t}^{in}$ and $f_{\ell,t}^{out}$ as well as the total line pack (inventory of gas) in each pipeline link at each time as $m_{\ell,t}$. With the defined terms, (4.15a) and (4.15b) are the mass and momentum equations, (4.15c), (4.15d), (4.15e), (4.15f) define the convenience variables for flow and pressure in and out of each pipeline, (4.15g) and (4.15h) prescribe the system to initially be at steady-state, and (4.15i) and (4.15j) define line pack and require each pipeline to refill its line pack by the end of the time horizon.

Capturing the space-time structure of (4.15) is seemingly complex but it is straightforward to do so with an OptiGraph because each pipeline can be treated independently. Code Snippet 14 in the Appendix details how each pipeline model is constructed.

$$\frac{p_{\ell,t+1,k} - p_{\ell,t,k}}{\Delta t} = -c_{1,\ell} \frac{f_{\ell,t+1,k+1} - f_{\ell,t+1,k}}{\Delta x_\ell}, \ell \in \mathcal{L}_p, t \in \bar{\mathcal{T}}, k \in \bar{\mathcal{X}}, \quad (4.15a)$$

$$\frac{f_{\ell,t+1,k} - f_{\ell,t,k}}{\Delta t} = -c_{2,\ell} \frac{p_{\ell,t+1,k+1} - p_{\ell,t+1,k}}{\Delta x_\ell} - c_{3,\ell} \frac{f_{\ell,t+1,k} |f_{\ell,t+1,k}|}{p_{\ell,t+1,k}}, \ell \in \mathcal{L}_p, t \in \bar{\mathcal{T}}, k \in \bar{\mathcal{X}} \quad (4.15b)$$

$$f_{\ell,t,N_x} = f_{\ell,t}^{out}, \quad \ell \in \mathcal{L}_p, t \in \mathcal{T} \quad (4.15c)$$

$$f_{\ell,t,1} = f_{\ell,t}^{in}, \quad \ell \in \mathcal{L}_p, t \in \mathcal{T} \quad (4.15d)$$

$$p_{\ell,t,N_x} = p_{\ell,t}^{out}, \quad \ell \in \mathcal{L}_p, t \in \mathcal{T} \quad (4.15e)$$

$$p_{\ell,t,1} = p_{\ell,t}^{in}, \quad \ell \in \mathcal{L}_p, t \in \mathcal{T} \quad (4.15f)$$

$$\frac{f_{\ell,1,k+1} - f_{\ell,1,k}}{\Delta x_\ell} = 0, \quad \ell \in \mathcal{L}_p, k \in \bar{\mathcal{X}} \quad (4.15g)$$

$$c_{2,\ell} \frac{p_{\ell,1,k+1} - p_{\ell,1,k}}{\Delta x_\ell} + c_{3,\ell} \frac{f_{\ell,1,k} |f_{\ell,1,k}|}{p_{\ell,1,k}} = 0, \quad \ell \in \mathcal{L}_p, k \in \bar{\mathcal{X}} \quad (4.15h)$$

$$m_{\ell,t} = \frac{A_\ell}{c^2} \sum_{k=1}^{N_x} p_{\ell,t,k} \Delta x_\ell, \quad \ell \in \mathcal{L}_p, t \in \mathcal{T} \quad (4.15i)$$

$$m_{\ell,N_t} \geq m_{\ell,1}, \quad \ell \in \mathcal{L}_p. \quad (4.15j)$$

Compressor OptiGraph

The compressor models are created analogously to the junction and pipeline models. We use an ideal isentropic formulation given by (4.16) where $\eta_{\ell,t}$, $p_{\ell,t}^{in}$, $p_{\ell,t}^{out}$, and $P_{\ell,t}$ are the compression ratio, suction pressure, discharge pressure, and horsepower respectively for compressor link ℓ at time t . We also define constant parameters, c_p , T , and γ for heat capacity, temperature and isentropic efficiency. The variables $f_{\ell,t,in}$ and $f_{\ell,t,out}$ are used for convenience to be consistent with the pipeline link formulation. The compressor graph construction is straightforward and is shown in Code Snippet 15 in the Appendix.

$$p_{\ell,t}^{out} = \eta_{\ell,t} p_{\ell,t}^{in}, \quad \ell \in \mathcal{L}_c, t \in \mathcal{T} \quad (4.16a)$$

$$P_{\ell,t} = c_p \cdot T \cdot f_{\ell,t} \left(\left(\frac{p_{\ell,t}^{out}}{p_{\ell,t}^{in}} \right)^{\frac{\gamma-1}{\gamma}} - 1 \right), \quad \ell \in \mathcal{L}_c, t \in \mathcal{T} \quad (4.16b)$$

$$f_{\ell,t} = f_{\ell,t}^{in} = f_{\ell,t}^{out}, \quad \ell \in \mathcal{L}_c, t \in \mathcal{T}. \quad (4.16c)$$

Network OptiGraph

The network structure of the model is induced using a high-level graph wherein we use linking constraints to express mass conservation around each junction and boundary conditions for pipeline and compressor links according to the formulation given by (4.17). Here, (4.17a) represents mass conservation at each junction j and (4.17b) and (4.17c) are the pipeline and compressor link boundary conditions. We also define $\theta_{rec(\ell),t}$ and $\theta_{snd(\ell),t}$ as the receiving and sending junction for each link $\ell \in \mathcal{L}$ at time t and we define $\mathcal{L}_{rec}(j)$ and $\mathcal{L}_{snd}(j)$ as the set of receiving and sending links to each junction j respectively. The final optimal control problem is given by (4.18) which seeks to minimize the total operating cost over the 24-hour period where α_ℓ is the compressor cost for compressor link ℓ and $\alpha_{j,d}$ is the gas delivery price for demand d on junction j . The

complete formulation includes all of the junction, pipeline, compressor, and network equations. Code Snippet 16 in the Appendix assembles the complete natural gas model.

$$\sum_{\ell \in \mathcal{L}_{rec}(j)} f_{\ell,t}^{out} - \sum_{\ell \in \mathcal{L}_{snd}(j)} f_{\ell,t}^{in} + \sum_{s \in \mathcal{S}_j} f_{j,s,t} - \sum_{d \in \mathcal{D}_j} f_{j,d,t} = 0, \quad j \in \mathcal{J}, t \in \mathcal{T} \quad (4.17a)$$

$$p_{\ell,t}^{in} = \theta_{rec(\ell),t}, \quad \ell \in \mathcal{L}, t \in \mathcal{T} \quad (4.17b)$$

$$p_{\ell,t}^{out} = \theta_{snd(\ell),t}, \quad \ell \in \mathcal{L}, t \in \mathcal{T} \quad (4.17c)$$

$$\min_{\substack{\{\eta_{\ell,t}, f_{j,d,t}\} \\ \ell \in \mathcal{L}_c, d \in \mathcal{D}_j, j \in \mathcal{J}, t \in \mathcal{T}}} \sum_{\substack{\ell \in \mathcal{L}_c \\ t \in \mathcal{T}}} \alpha_{\ell} P_{\ell,t} - \sum_{\substack{d \in \mathcal{D}_j, j \in \mathcal{J}, \\ t \in \mathcal{T}}} \alpha_{j,d} f_{j,d,t} \quad (4.18a)$$

$$s.t. \quad \text{Junction Limits} \quad (4.14) \quad (4.18b)$$

$$\text{Pipeline Dynamics} \quad (4.15) \quad (4.18c)$$

$$\text{Compressor Equations} \quad (4.16) \quad (4.18d)$$

$$\text{Network Link Equations} \quad (4.17) \quad (4.18e)$$

Partitioning and Solving the Natural Gas Problem

Once we have constructed a graph representation of the problem, we can use the `Plasmo.jl` tools to explore different partitioning strategies. Figure 19 visualizes the graph structure of the problem and shows different partitions. Figure 19a shows the graph components we assembled in the above snippets with pipeline nodes depicted in grey, compressor nodes in green, and junctions in blue. Figure 19b depicts a pure time partition of the problem with 8 partitions (each with a different color). Partitioning in time is an intuitive approach but this results in 87,505 linking constraints (making the Schur matrix intractable). This problem can also be partitioned purely as a network wherein we consider the partition of the network components themselves (as opposed to the structure of the problem) which is shown in Figure 19c. The network partition is physically intuitive but it does not capture the true mathematical structure of the problem nor consider load balancing. We highlight that both time and network partitioning approaches can be performed using the partitioning framework (by manually defining a partition vector), but the value of having the graph is that we can efficiently obtain space-time partitions to produce the partition shown in Figure 19d. While visually similar to the network partition, the space-time partition produces considerably less coupling (748 linking constraints against 1,800 linking constraints), thus leading to a small Schur matrix. We also highlight that the space-time partition requires traversing space-time.

Code Snippet 11 shows how to partition the gas network problem and produce the problem we communicate to `PIPS-NLP`. Line 2 imports the `KaHyPar` hypergraph partitioner, Line 5 formulates the hypergraph representation of our problem, and Lines 8 through 10 setup weight vectors we use for the nodes and edges (we weight nodes by their number of variables and edges by their number of linking constraints). We partition the hypergraph on Line 14, create a `Partition` object on Line 17, produce new subgraphs on Line 20 and finally aggregate the subgraphs on Line 23.

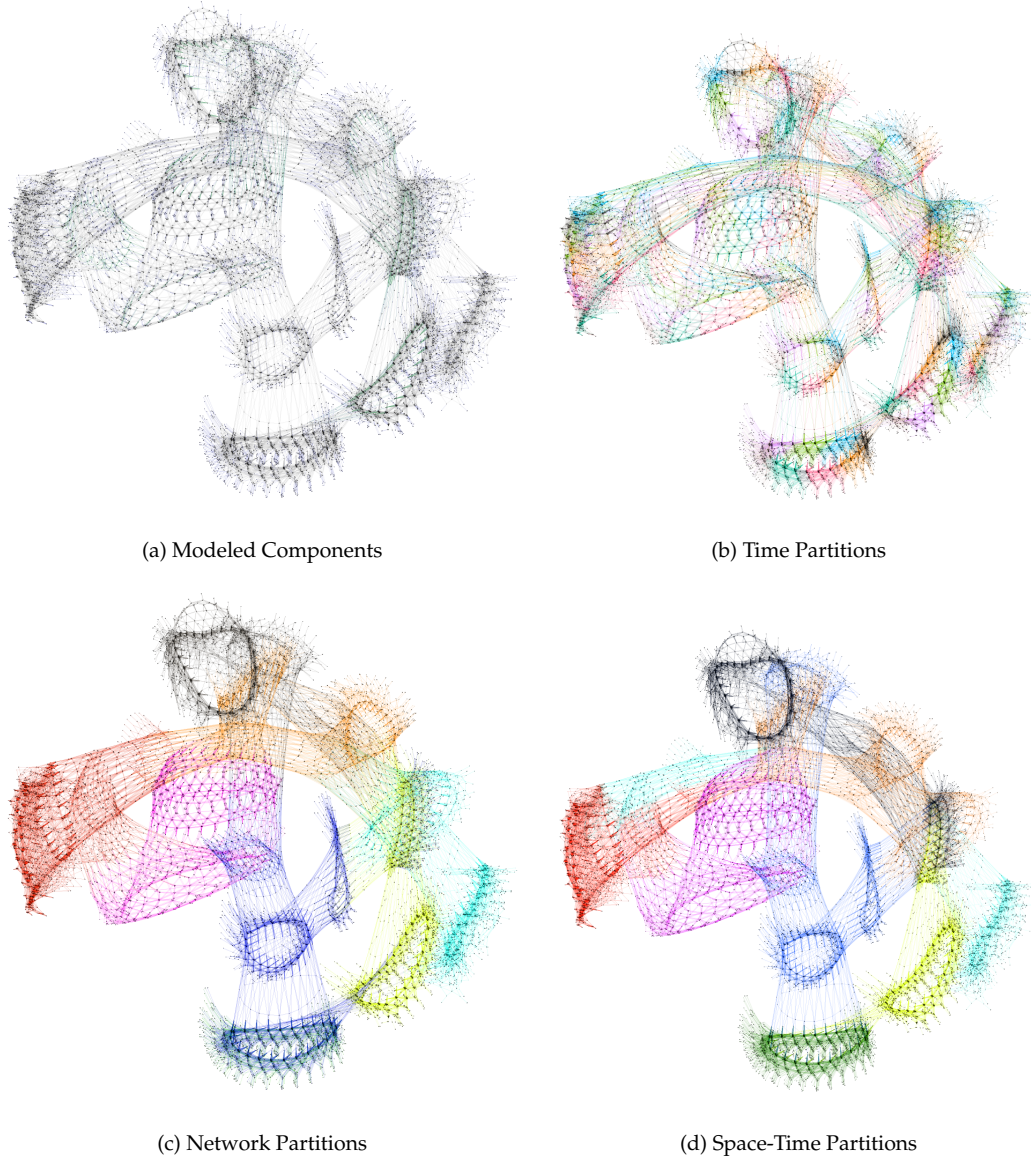


Fig. 19: Graph layouts of the natural gas network problem. The graph is colored by the physical network components (top left), by 8 time partitions (top right), by 8 network partitions (bottom left), and by 8 space-time partitions (bottom right).

Code Snippet 11: Partitioning the gas network control problem

```

1  #Import the KaHyPar interface
2  using KaHyPar
3
4  #Get they hypergraph representation of the gas network
5  hypergraph, ref_map = gethypergraph(gas_network)
6
7  #Setup node and edge weights
8  n_vertices = length(vertices(hypergraph))
9  node_weights = [num_variables(node) for node in all_nodes(gas_network)]
10 edge_weights = [num_link_constraints(edge) for edge in all_edges(gas_network)]
11
12 #Use KaHyPar to partition the hypergraph
13 node_vector = KaHyPar.partition(hypergraph, 8, configuration = :edge_cut,
14 imbalance = 0.01, node_weights = node_weights, edge_weights = edge_weights)
15
16 #Create a model partition
17 partition = Partition(gas_network, node_vector, ref_map)
18
19 #Setup subgraphs based on partition
20 make_subgraphs!(gas_network, partition)
21
22 #Aggregate the subgraphs into OptiNodes
23 new_graph , aggregate_map = aggregate(gas_network, 0)

```

The partitioning in Snippet 11 produces a graph with 8 nodes which we can distribute and solve with PIPS-NLP. We follow the exact same setup used in Snippet 9 using `PipsSolver.jl` and distribute the graph between workers to solve in parallel on a machine with 32 Intel Xeon CPUs E5-2698 v3 running at 2.30 GHz. We experiment with different numbers of partitions and imbalance values and explore how the PIPS-NLP algorithm performs. Table 3 details the results obtained where we vary the number of partitions $|\mathcal{P}|$ (8, 24, and 48) and the maximum imbalance value ϵ_{max} (between 0.01 and 1.0). Figure 20 shows the effect of increasing the imbalance for the 48 partition case on the true final imbalance the partitioner produced (ϵ_{final}) and the total number of linking constraints. For the most part, the maximum and final imbalances ϵ_{final} display a one-to-one relationship but there are distinct intervals wherein the final imbalance flattens out. We also see that nominal values of maximum imbalance (less than 25%) reduce the number of linking constraints considerably but greater values produce diminishing returns. Here, we also show the distribution of subproblem sizes for a few select maximum imbalance values on the right side of Figure 20 for reference. We can see that, under naive partitioning, the size of the partitions can vary by an order of magnitude.

For each run, we note the true imbalance KaHyPar produced ϵ_{final} , the sum of the edge weights $sum(w(\mathcal{E}))$ (which corresponds to the number of linking constraints), the maximum node size $max(\{s(n)\}_{n \in \mathcal{N}(\mathcal{G})})$ (which corresponds to the node with the most variables), as well as the average and maximum number of node connections (i.e. the number of linking constraints incident to a node). For timing results we observe the time spent building the KKT system t_{build} (i.e. the time to build (3.10b)), the time spent factorizing the Schur complement t_{fac} (i.e. time to solve (3.10b)) and the total time spent inside PIPS-NLP t_{pips} . The first rows of Table 3 show results with 8 partitions and also include cases for time and network partitions corresponding to Figures 19b and 19c. As expected, the high degree of coupling in these partitions is computationally prohibitive; the time partition cannot be solved with Schur complement decomposition and the network partition requires over 2 hours. Significant improvement is achieved by using the KaHyPar partitioner; we note that even a 1% imbalance is twice as fast as the network partition. Increasing the imbalance parameter to 50% results in much better performance (the average and maximum number of columns in B_n decreases), but increasing it to 60% results in diminished speed, despite producing

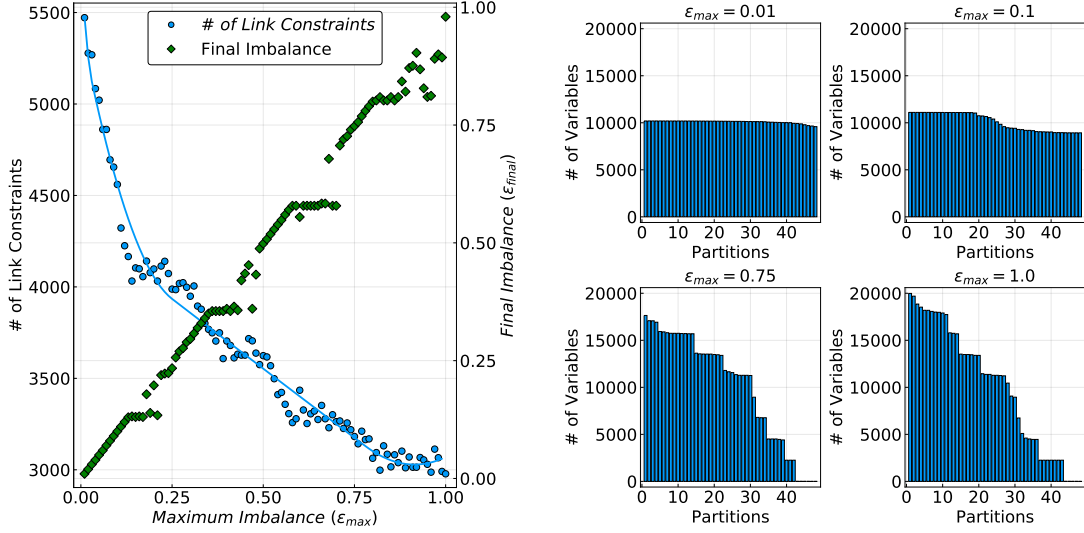


Fig. 20: Partitioning results with 48 partitions. Imbalance versus the number of linking constraints and final imbalance (left) and the distribution of subproblem sizes for select imbalance parameters (right).

a similar partition. Interestingly, allowing too much imbalance can result in ill-conditioned subproblems (e.g., ill-conditioned matrices K_n). This highlights why having flexibility in partitioning is important. The second and third sets of rows present the results using 24 and 48 partitions with 24 CPUs. Increasing the maximum imbalance for the 24 partition case results in diminished performance (due to the bottleneck of building the KKT system). This is because either the node connectivity increases (for the 10% imbalance), the maximum subproblem size increases (for the 100% imbalance), or there is some ill-conditioning of the subproblems. In contrast, increasing the imbalance for the 48 partition case results in computational improvement. This is because more linking constraints (more coupling) shifts the bottleneck step to factorizing the Schur complement and drastic speedups result from reducing the degree of coupling. This highlights how flexible partitions can help fit the solver to the computing architecture of interest.

4.2 Overlapping Schwarz Decomposition for DC OPF

This case study demonstrates how we can use graph partitioning and topology manipulation to pose a complex power network problem to the Schwarz overlapping scheme. We consider a 9,241 bus test case obtained from `pglib-opf` (v19.05) [4], which we obtain through `Power-Models.jl` [14]. We denote the power grid as a network $Net(\mathcal{V}, \mathcal{L}_{grid})$ containing a set of electric buses \mathcal{V} that connect power lines $\ell \in \mathcal{L}_{grid}$. Each electric bus $i \in \mathcal{V}$ can include generators $q \in \Omega_i$ and serves a total power load P_i^L . The total set of generators is given by Ω such that $\bigcup_{i \in \mathcal{V}} \Omega_i = \Omega$. The network is described by the DC power flow equations [76] given by (4.19) where (4.19a) seeks to minimize the total generation cost and voltage angle difference where β is a regularization

Partition	ϵ_{max}	ϵ_{final}	$\sum_{e \in \mathcal{E}(\mathcal{G})} (w(e))$ (# Link Constraints)	$max(\{s(n)\}_{n \in \mathcal{N}(\mathcal{G})})$ (Largest node)	$\{\sum_{e \in \mathcal{E}(n)} (w(e))\}_{n \in \mathcal{N}(\mathcal{G})}$ (# Incident Node Links) mean, max	t_{build} (sec)	t_{fac} (sec)	t_{pips} (sec)
\mathcal{P} = 8 # Proc = 8	time	0.0	87505	60567	21877, 24940	-	-	-
	network	0.41	1800	85248	459, 1368	7236	56	7505
	0.01	0.0073	748	61008	205, 316	2944	6.3	3115
	0.5	0.37	434	83202	121, 218	2269	1.7	2475
	0.6	0.37	458	83202	124, 218	2862	1.9	3069
\mathcal{P} = 24 # Proc = 24	0.01	0.01	2889	20390	259, 431	1746	273	2117
	0.1	0.1	2748	22200	256, 529	1934	236	2270
	1.0	0.99	1572	40080	127, 362	2279	54	2447
\mathcal{P} = 48 # Proc = 24	0.01	0.01	5472	10194	245, 482	2029	1769	3954
	0.1	0.1	4560	11104	210, 440	1871	1031	3054
	0.75	0.75	3182	17642	151, 387	2126	368	2670
	1.0	0.98	2978	19985	143, 480	1826	298	2247

Table 3: PIPS-NLP results for different graph partitions.

parameter. (4.19b) enforces energy conservation, and (4.19e) and (4.19f) denote limits on power generation and voltage angles. In this formulation, v_i is the bus voltage angle for each bus $i \in \mathcal{V}$, P_q is the power generation from generator q with cost coefficients $c_{q,1}$ and $c_{q,2}$ and lower and upper limits \underline{P}_q and \overline{P}_q , and $v_{\ell,j}$ and $v_{\ell,k}$ are the inlet and outlet voltage angles on ℓ with ramp limit \overline{v}_ℓ . We also define $\mathcal{L}_{rec}(i)$ as the set of power links received by bus i and $\mathcal{L}_{snd}(i)$ as the set of links sent from bus i . The power flow on line ℓ is defined by (4.19d), where Y_ℓ is the branch admittance for line ℓ , $v_{\ell,j}$ is the source bus voltage angle and $v_{\ell,k}$ is the destination bus voltage angle. $src(\ell)$ denotes the source bus of line ℓ and $dst(\ell)$ is destination bus for line ℓ . We denote the voltage angles on the set of reference buses in (4.19g) where \mathcal{V}^{ref} is the set of reference buses.

$$\min_{\substack{\{v_i\}_{i \in \mathcal{V}} \\ \{P_q\}_{q \in \Omega}}} \sum_{q \in \Omega} (c_{q,1} P_q + c_{q,2} P_q^2) + \frac{\beta}{2} \sum_{\ell \in \mathcal{L}_{grid}} (v_{\ell,j} - v_{\ell,k})^2 \quad (4.19a)$$

$$s.t. \sum_{q \in \Omega_i} P_q + \sum_{\ell \in \mathcal{L}_{rec}(i)} P_\ell - \sum_{\ell \in \mathcal{L}_{snd}(i)} P_\ell = P_i^L, \quad i \in \mathcal{V} \quad (4.19b)$$

$$v_{\ell,j} = v_{src(\ell)}, v_{\ell,k} = v_{dst(\ell)}, \quad \ell \in \mathcal{L}_{grid} \quad (4.19c)$$

$$P_\ell = Y_\ell (v_{\ell,j} - v_{\ell,k}), \quad \ell \in \mathcal{L}_{grid} \quad (4.19d)$$

$$\underline{P}_q \leq P_q \leq \overline{P}_q, \quad q \in \Omega \quad (4.19e)$$

$$-\overline{v}_\ell \leq v_{\ell,j} - v_{\ell,k} \leq \overline{v}_\ell, \quad \ell \in \mathcal{L}_{grid} \quad (4.19f)$$

$$v_i = v_i^{ref}, \quad i \in \mathcal{V}^{ref} \quad (4.19g)$$

We construct the DC OPF model with Code Snippet 17, which produces an optimization problem with over 100,000 variables and constraints. The DC OPF model is partitioned using `KaHyPar`; once we obtain partitions, we create subgraphs, expand them, and solve the problem using the `SchwarzSolver.jl`. Code Snippet 12 demonstrates how we carry this out using a maximum imbalance of 10% and an overlap size of $\omega = 10$. Line 1 imports `KaHyPar` and Line 6 creates a hypergraph and `ref_map` which we use for partitioning. Lines 9 through 11 query the graph for edge weights and node sizes, Line 15 partitions the DC OPF problem, and Lines 18 and 21 create a `Partition` and use it to define subgraphs for the problem. Once we have subgraphs, we perform a subgraph expansion on Line 27 and execute the Schwarz solver on Line 31. We also show how to

tell the solver how to treat linking constraints. We provide the keyword argument `primal_links` with the vector of power flow linking constraints and we provide the keyword `dual_links` with a vector of voltage angle linking constraints to denote how subproblems are formulated; the constraints that are specified as `primal_links` are treated as direct constraints while the constraints in `dual_links` are incorporated as dual penalty as described in (3.11).

Code Snippet 12: Partitioning and Formulating Overlapping Subproblems

```

1  using KaHyPar
2  using Ipopt
3  using SchwarzSolver
4
5  #Get the hypergraph representation of the gas network
6  hypergraph,ref_map = gethypergraph(dcopf)
7
8  #Setup node and edge weights
9  n_vertices = length(vertices(hypergraph))
10 node_weights = [num_variables(node) for node in all_nodes(dcopf)]
11 edge_weights = [num_link_constraints(edge) for edge in all_edges(dcopf)]
12
13 #Use KaHyPar to partition the hypergraph
14 node_vector = KaHyPar.partition(hypergraph,4,configuration = :edge_cut,
15 imbalance = 0.1, node_weights = node_weights,edge_weights = edge_weights)
16
17 #Create a partition object
18 partition = Partition(dcopf,node_vector,ref_map)
19
20 #Setup subgraphs based on partition
21 make_subgraphs!(dcopf,partition)
22
23 distance = 10
24 subgraphs = getsubgraphs(dcopf)
25
26 #Expand the subgraphs
27 sub_expand = expand.(Ref(dcopf),subgraphs,Ref(distance))
28
29 ipopt = Ipopt.Optimizer
30
31 schwarz_solve(dcopf,sub_expand,primal_links = power_links,
32 dual_links = [angle_i;angle_j]),
33 sub_optimizer = ipopt,max_iterations = 100,tolerance = 1e-3)

```

Figure 21 depicts the original and overlapping partitions obtained from Snippet 12. These are visualized using Gephi. We experiment with different values for maximum imbalance and overlap and obtain the results in Figure 22. We see that the Schwarz algorithm fails to converge with an overlap value of one (for any imbalance value) which is consistent with the convergence analysis in [70], but a sufficient overlap of 10 produces smooth convergence (for each imbalance value). We also found that larger partition imbalance results in faster convergence (with sufficient overlap) which is likely due to the smaller edge cut and fewer linking constraints that need to be satisfied. We thus see that the trade-offs of imbalance and coupling are complex and differ under different problems and algorithms.

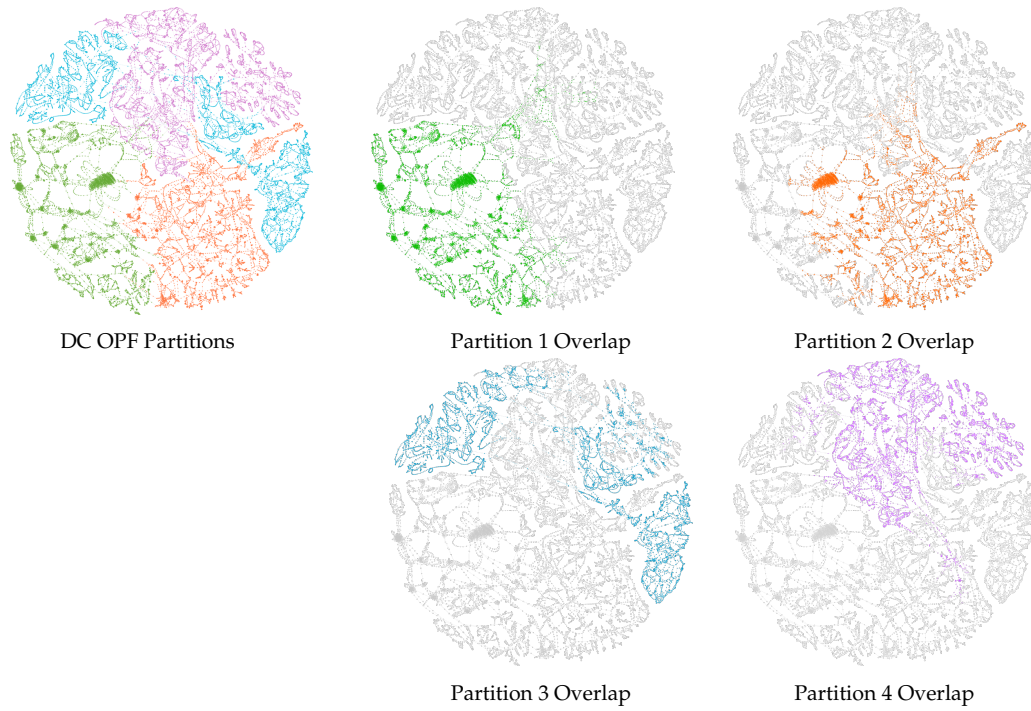


Fig. 21: Depiction of DC OPF problem with four partitions. The original calculated partitions with $\epsilon_{max} = 0.1$ (left) and the corresponding overlap partitions with $\omega = 10$ (right).

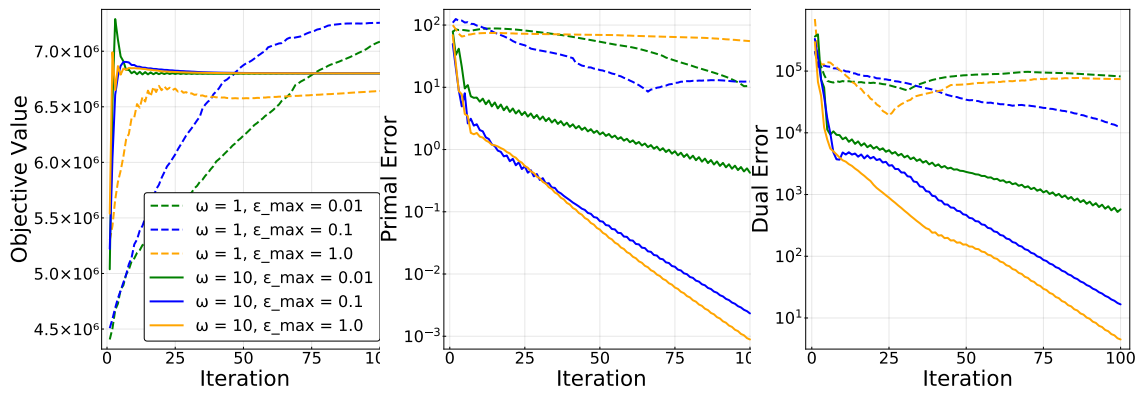


Fig. 22: Comparison of Schwarz algorithm for different values of overlap ω and maximum partition imbalance ϵ_{max}

5 Outlook and Extensions for `Plasmo.jl`

We presented a graph-based modeling abstraction for optimization that we call an `OptiGraph`. We showcased its implementation in `Plasmo.jl` and demonstrated how this provides flexibility to use different graph analysis and visualization tools. We also showed how these capabilities facilitate the use of decomposition strategies at both the linear algebra and problem levels. There are broad opportunities to refine and expand the capabilities of the proposed abstraction and of `Plasmo.jl`. The most evident next step is to develop interfaces to a wider range of decomposition solvers. As such, we are currently developing interfaces to `DSP` [47] (a Benders and Lagrangian dual decomposition solver for stochastic optimization), and `SNGO` [11] (a Julia-based global solver for nonlinear stochastic programs). We are also interested in new parallel interior point solvers that use recent Schur decomposition strategies to solve massive energy system models [62]. In this regard, the graph could be a natural interface for `BELTISTOS` [48], a nonlinear solver that exploits specialized time decomposition structures that arise in Schur decomposition. These capabilities will enable solution of a wide range of application problems.

As ongoing work we are also developing *parallel modeling* capabilities to create graph objects in parallel. Parallel modeling becomes important in instances when the model itself is too large to fit in memory, such as with stochastic programs with many scenarios. Scenario-based optimization problems have been modeled in parallel using `StructJuMP` and `MPI`, but more complex structures (such as those with many linking constraints) are more challenging to implement in a parallel modeling framework. In this context, the Parallel Structured Model Generator (`PSMG`) [29] is the only framework we know of that performs parallel model generation which works with structured conveying modeling language (`SML`) [15]. `PSMG` focuses on efficient distributed memory design to achieve parallel generation, but it requires solvers to perform subproblem distribution and load balancing based on a well-defined model structure. In contrast, we hope to facilitate the modeling, partitioning, and parallel generation tasks in a more systematic interactive framework using the `OptiGraph`.

Finally, we demonstrated how to partition graphs using powerful tools such as `Metis` and `KaHyPar`. Exploiting such graph partitioning tools opens many possibilities for using decomposition-based solvers, but it is limited to expressing problem characteristics strictly in the form of edge weights and node sizes. We are interested in developing more customized graph partitioning algorithms that work directly on the graph attributes (such as accounting for integer variables). We are also interested in developing algorithms that calculate overlap directly as opposed to performing subgraph expansion. Such modeling advances can provide new capabilities that open diverse algorithmic development and offer interesting directions for future research.

Acknowledgements

This material is based on work supported by the U.S. Department of Energy (DOE), Office of Science, under Contract No. DE-AC02-06CH11357 as well as the DOE Office of Electricity Delivery and Energy Reliability's Advanced Grid Research and Development program (AGR&D). This work was also partially supported by the U.S. Department of Energy grant DE-SC0014114. We also acknowledge partial support from the National Science Foundation under award NSF-EECS-1609183. The authors acknowledge Yankai Cao for his work developing the original `PiPS-NLP` interface for `Plasmo.jl`. The authors also acknowledge Michel Schanen from Argonne National

Laboratory for his assistance using and debugging PIPS-NLP as well as Kibaek Kim from Argonne National Laboratory for his help in the conceptualization of `Plasmo.jl`.

Appendix: Code Snippets

Junction OptiGraph Implementation

The junction `OptiGraph` is implemented in Code Snippet 13. We define the function `create_junction_model` on Line 2 which accepts junction specific data and the number of time periods `nt`. We create the `OptiGraph` `graph` on Lines 3 through 26 where we add a node for each time interval and then create the variables and constraints for each node in a loop. We also use the JuMP specific `@expression` macro to refer to expressions for total gas supplied, total gas delivered, and total cost for convenience. The junction model is returned from the function on Line 29.

Code Snippet 13: Creating a gas junction graph

```

1  #Define function to create junction OptiGraph
2  function create_junction_model(data,nt)
3      graph = OptiGraph()
4
5      #Add OptiNode for each time interval
6      @optinode (graph,nodes[1:nt])
7
8      #query number of supply and demands on the junction
9      n_demands = length(data[:demand_values])
10     n_supplies = length(data[:supplies])
11
12     #Loop and create variables, constraints, and objective for each OptiNode
13     for (i,node) in enumerate(nodes)
14         @variable (node, data[:pmin] <= pressure <= data[:pmax], start = 60)
15         @variable (node, 0 <= fgen[1:n_supplies] <= 200, start = 10)
16         @variable (node, fdeliver[1:n_demands] >= 0)
17         @variable (node, fdemand[1:n_demands] >= 0)
18
19         @constraint (node, [d = 1:n_demands],fdeliver[d] <= fdemand[d])
20
21         @expression (node, total_supplied, sum(fgen[s] for s = 1:n_supplies))
22         @expression (node, total_delivered, sum(fdeliver[d] for d = 1:n_demands))
23         @expression (node, total_delivercost, sum(1000*fdeliver[d] for d = 1:n_demands))
24
25         @objective (node,Min,total_delivercost)
26     end
27
28     #Return the graph
29     return graph
30 end

```

Pipeline OptiGraph Implementation

The pipeline `OptiGraph` is given by Code Snippet 14. We again use a function (`create_pipeline_model`) to create the graph and we unpack the input data and create nodes, variables, and constraints on Lines 3 through 25. We define the set of `OptiNodes` on Line 10 as `grid`, which we use to refer to `OptiNodes` using time and space indices. To capture the space-time coupling of each pipeline we use linking constraints on Lines 28 through 42 to define the finite difference scheme, the steady-state condition, and the line pack constraint.

Code Snippet 14: Creating a pipeline graph

```

1  function create_pipeline_model(data, nt, nx)
2      #Unpack data
3      c1 = data[:c1]; c2 = data[:c2]; c3 = data[:c3]
4      dx = data[:pipe_length] / (nx - 1)
5
6      #Create pipeline OptiGraph
7      graph = OptiGraph()
8
9      #Create grid of OptiNodes
10     @optinode(graph, grid[1:nt, 1:nx])
11
12     #Create variables on each node in the grid
13     for node in grid
14         @variable(node, 1 <= px <= 100)
15         @variable(node, 0 <= fx <= 100)
16         @variable(node, slack >= 0)
17         @NLnodeconstraint(node, slack*px - c3*fx*fx == 0)
18     end
19
20     #Setup dummy variable referenes
21     @expression(graph, fin[t=1:nt], grid[:, 1][t][:fx])
22     @expression(graph, fout[t=1:nt], grid[:, end][t][:fx])
23     @expression(graph, pin[t=1:nt], grid[:, 1][t][:px])
24     @expression(graph, pout[t=1:nt], grid[:, end][t][:px])
25     @expression(graph, linepack[t=1:nt], c2/A*sum(grid[t, x][:px]*dx for x in 1:nx-1))
26
27     #Finite differencing. Backward difference in time from t, Forward difference in space from x.
28     @linkconstraint(graph, press[t=2:nt, x=1:nx-1],
29         (grid[t, x][:px]-grid[t-1, x][:px])/dt +
30         c1*(grid[t, x+1][:fx] - grid[t, x][:fx])/dx == 0)
31
32     @linkconstraint(graph, flow[t=2:nt, x=1:nx-1], (grid[t, x][:fx] -
33         grid[t-1, x][:fx])/dt == -c2*(grid[t, x+1][:px] -
34         grid[t, x][:px])/dx - grid[t, x][:slack])
35
36     #Initial steady state
37     @linkconstraint(graph, ssflow[x=1:nx-1], grid[1, x+1][:fx] - grid[1, x][:fx] == 0)
38     @linkconstraint(graph, sspress[x = 1:nx-1], -c2*(grid[1, x+1][:px] -
39         grid[1, x][:px])/dx - grid[1, x][:slack] == 0)
40
41     #Refill pipeline line pack
42     @linkconstraint(graph, linepack[end] >= linepack[1])
43     return graph
44 end

```

Compressor OptiGraph Implementation

The compressor `OptiGraph` construction is fairly straight-forward and given by 15. Line 1 defines the function `create_compressor_model` which takes `data` and the number of time periods `nt`. Line 3 creates the `OptiGraph` for the compressor model, Line 4 creates an `OptiNode` for each time point, and Lines 7 through 15 define the model variables and constraints. Lines 19 and 20 define helpful expressions for the flow in and out of the compressor and Line 23 returns the `OptiGraph`.

Code Snippet 15: Creating a compressor graph

```

1  function create_compressor_model(data,nt)
2  #Create compressor OptiGraph
3  graph = OptiGraph()
4  @optinode(graph,nodes[1:nt])
5
6  #Setup variables, constraints, and objective
7  for node in nodes
8      @variable(node, 1 <= psuction <= 100)
9      @variable(node, 1 <= pdischarge <= 100)
10     @variable(node, 0 <= power <= 1000)
11     @variable(node, flow >= 0)
12     @variable(node, 1 <= eta <= 2.5)
13     @NLnodeconstraint(node, pdischarge == eta*psuction)
14     @NLnodeconstraint(node, power == c4*flow*((pdischarge/psuction)^om-1) )
15     @objective(node, Min, cost*power*(dt/3600.0))
16 end
17
18 #Create references for flow in and out
19 @expression(graph,fin[t=1:nt],nodes[t][:flow])
20 @expression(graph,fout[t=1:nt],nodes[t][:flow])
21
22 #Return compressor OptiGraph
23 return graph
24 end

```

Network OptiGraph Implementation

The network `OptiGraph` couples the other component graphs at a higher level and is implemented in Code Snippet 16. We create the graph `gas_network` on Line 2 and add the component subgraphs on Lines 5 through 13. Once we have the multi-level subgraph structure we create linking constraints at the `gas_network` level on Lines 16 through 46 which impose the junction conservation and boundary conditions for the network links (pipelines and compressors).

Code Snippet 16: Formulating the complete gas network graph

```

1  #Create OptiGraph for entire gas network
2  gas_network = OptiGraph()
3
4  #Add every device graph to the network
5  for pipe in pipelines
6      add_subgraph!(gas_network,pipe)
7  end
8  for compressor in compressors
9      add_subgraph!(gas_network,compressor)
10 end
11 for junction in junctions
12     add_subgraph!(gas_network,junction)
13 end
14
15 #Link pipelines in gas network
16 for pipe in pipelines
17     junction_from,junction_to = pipe_map[pipe]
18     @linkconstraint(gas_network,[t = 1:nt],pipe[:pin][t] ==
19     junction_from[:pressure][t])
20     @linkconstraint(gas_network,[t = 1:nt],pipe[:pout][t] ==
21     junction_to[:pressure][t])
22 end
23
24 #Link compressors in gas network
25 for compressor in compressors
26     junction_from,junction_to = compressor_map[compressor]
27     @linkconstraint(gas_network,[t = 1:nt],compressor[:pin][t] ==
28     junction_from[:pressure][t])
29     @linkconstraint(gas_network,[t = 1:nt],compressor[:pout][t] ==
30     junction_to[:pressure][t])
31 end
32
33 #Link junctions in gas network
34 for junction in junctions
35     devices_in = junction_map_in[junction]
36     devices_out = junction_map_out[junction]
37
38     flow_in = [sum(device[:fout][t] for device in devices_in) for t = 1:nt]
39     flow_out = [sum(device[:fin][t] for device in devices_out) for t = 1:nt]
40
41     total_supplied = [junction[:total_supplied][t] for t = 1:nt]
42     total_delivered = [junction[:total_delivered][t] for t = 1:nt]
43
44     @linkconstraint(gas_network,[t = 1:nt], flow_in[t] - flow_out[t] +
45     total_supplied[t] - total_delivered[t] == 0)
46 end

```

DC OPF Model Implementation

The DC optimal power flow model is implemented in Code Snippet 17. Line 1 loads the bus system using `PowerModels.jl`, Line 4 creates the graph, Lines 7 and 8 create nodes for each bus and line in the network, and Line 11 assigns relevant data to each bus and line node using a `load_data!` function. The DC OPF model is constructed in the same fashion as described in earlier examples where Lines 14 through 55 setup models on each node and add linking constraints corresponding to power conservation and voltage angle connections.

Code Snippet 17: Creating the DC OPF Problem

```

1  include("ogplib_data.jl")
2
3  #Create graph based on network
4  grid = OptiGraph()
5
6  #Create bus and power line nodes
7  @optinode (grid,buses[1:N_buses])
8  @optinode (grid,lines[1:N_lines])
9
10 #Load data and setup bus and line mappings
11 load_data!(lines,buses)
12
13 #Setup line OptiNodes
14 for line in lines
15     bus_from = line_map[line][1]
16     bus_to = line_map[line][2]
17     delta = line.ext[:angle_rate]
18     @variable (line,va_i,start = 0)
19     @variable (line,va_j,start = 0)
20     @variable (line,flow,start = 0)
21     @constraint (line,flow == B[line]*(va_i - va_j))
22     @constraint (line,delta <= va_i - va_j <= -delta)
23     @objective (line,Min,gamma*(va_i - va_j)^2)
24 end
25
26 #Setup bus OptiNodes
27 power_links = []
28 for bus in buses
29     va_lower = bus.ext[:va_lower]; va_upper = bus.ext[:va_upper]
30     gen_lower = bus.ext[:gen_lower]; gen_upper = bus.ext[:gen_upper]
31
32     @variable (bus,va_lower <= va <= va_upper)
33     @variable (bus,P[j=1:ngens[bus]])
34     @constraint (bus,[j = 1:ngens[bus]]gen_lower[j] <= P[j] <= gen_upper[j])
35
36     lines_in = node_map_in[bus] ; lines_out = node_map_out[bus]
37
38     @variable (bus,power_in[1:length(lines_in)])
39     @variable (bus,power_out[1:length(lines_out)])
40
41     @constraint (bus,power_balance, sum(bus[:P][j] for j=1:ngens[bus]) -
42 sum(power_in) + sum(power_out) - load_map[bus] == 0)
43     @objective (bus,Min,sum(bus.ext[:c1][j]*bus[:P][j] +
44 bus.ext[:c2][j]*bus[:P][j]^2 for j = 1:ngens[bus]))
45
46 #Link power flow
47 p1 = @linkconstraint (grid,[j = 1:length(lines_in)],
48 bus[:power_in][j] == lines_in[j][:flow])
49 p2 = @linkconstraint (grid,[j = 1:length(lines_out)],
50 bus[:power_out][j] == lines_out[j][:flow])
51 push!(power_links,p1) ; push!(power_links,p2)
52 end
53
54 #Link voltage angles
55 @linkconstraint (grid,angle_i[line = lines],line[:va_i] ==
56 line_map[line][1][:va])
57 @linkconstraint (grid,angle_j[line = lines],line[:va_j] ==
58 line_map[line][2][:va])

```

References

1. ABHYANKAR, S., BROWN, J., CONSTANTINESCU, E. M., GHOSH, D., SMITH, B. F., AND ZHANG, H. Petsc/ts: A modern scalable ode/dae solver library. *arXiv preprint arXiv:1806.01437* (2018).
2. ALLMAN, A., TANG, W., AND DAOUTIDIS, P. Towards a Generic Algorithm for Identifying High-Quality Decompositions of Optimization Problems. In *Computer Aided Chemical Engineering*. 2018.
3. ALLMAN, A., TANG, W., AND DAOUTIDIS, P. Decode: a community-based algorithm for generating high-quality decompositions of optimization problems. *Optimization and Engineering* (06 2019).
4. BABAEINEJADSAROOKOLAE, S., BIRCHFIELD, A., CHRISTIE, R. D., COFFRIN, C., DEMARCO, C., DIAO, R., FERRIS, M., FLISCOUNAKIS, S., GREENE, S., HUANG, R., JOSZ, C., KORAB, R., LESIEUTRE, B., MAEGHT, J., MOLZAHN, D. K., OVERBYE, T. J., PANCIATICI, P., PARK, B., SNODGRASS, J., AND ZIMMERMAN, R. The power grid library for benchmarking ac optimal power flow algorithms, 2019.
5. BASTIAN, M., HEYMANN, S., AND JACOMY, M. Gephi: An open source software for exploring and manipulating networks, 2009.
6. BERGNER, M., CAPRARA, A., CESELLI, A., FURINI, F., LÜBBECKE, M. E., MALAGUTI, E., AND TRAVERSI, E. Automatic dantzig-wolfe reformulation of mixed integer programs. *Mathematical Programming* 149, 1 (feb 2015), 391–424.
7. BIEL, M., AND JOHANSSON, M. Efficient stochastic programming in julia, 2019.
8. BOYD, S., PARIKH, N., CHU, E., PELEATO, B., AND ECKSTEIN, J. Distributed optimization and statistical learning via the alternating direction method of multipliers. *Found. Trends Mach. Learn.* 3, 1 (Jan. 2011), 1122.
9. BRUNAUD, B., AND GROSSMANN, I. E. Perspectives in multilevel decision-making in the process industry. *Frontiers of Engineering Management* 4, 3 (2017), 1–34.
10. CAO, Y., FUENTES-CORTES, L. F., CHEN, S., AND ZAVALA, V. M. Scalable modeling and solution of stochastic multi-objective optimization problems. *Computers & Chemical Engineering* 99 (2017), 185–197.
11. CAO, Y., AND ZAVALA, V. M. A scalable global optimization algorithm for stochastic nonlinear programs.
12. ÇATALYÜREK, Ü., AND AYKANAT, C. *PaToH (Partitioning Tool for Hypergraphs)*. Springer US, Boston, MA, 2011, pp. 1479–1487.
13. CHIANG, N. Y., AND ZAVALA, V. M. Large-scale optimal control of interconnected natural gas and electrical transmission systems. *Applied Energy* 168 (2016), 226–235.
14. COFFRIN, C., BENT, R., SUNDAR, K., NG, Y., AND LUBIN, M. Powermodels.jl: An open-source framework for exploring power flow formulations. In *2018 Power Systems Computation Conference (PSCC)* (June 2018), pp. 1–8.
15. COLOMBO, M., GROTHEY, A., HOGG, J., WOODSEND, K., AND GONDZIO, J. A structure-conveying modelling language for mathematical and stochastic programming. *Mathematical Programming Computation* (2009).
16. CONEJO, A. J., CASTILLO, E., MÍNGUEZ, R., AND GARCÍA-BERTRAND, R. *Decomposition techniques in mathematical programming: Engineering and science applications*. 2006.
17. DEVINE, K. D., BOMAN, E. G., HEAPHY, R. T., BISSELING, R. H., AND CATALYUREK, U. V. Parallel hypergraph partitioning for scientific computing. In *20th International Parallel and Distributed Processing Symposium, IPDPS 2006* (2006).
18. DOWLING, A. W., AND BIEGLER, L. T. A framework for efficient large scale equation-oriented flowsheet optimization. *Computers & Chemical Engineering* 72 (2015), 3–20.
19. DUNNING, I., HUCHETTE, J., AND LUBIN, M. Jump: A modeling language for mathematical optimization. *SIAM Review* 59, 2 (2017), 295–320.
20. FARINA, F., CAMISA, A., TESTA, A., NOTARNICOLA, I., AND NOTARSTEFANO, G. Disropt : a python framework. 1–14.
21. FERRIS, M. C., AND HORN, J. D. Partitioning mathematical programs for parallel solution. *Mathematical Programming* 80, 1 (jan 1998), 35–61.
22. FISHER, M. L. APPLICATIONS ORIENTED GUIDE TO LAGRANGIAN RELAXATION. *Interfaces* (1985).
23. FOURER, R., GAY, D. M., AND KERNIGHAN, B. *AMPL: A Mathematical Programming Language*. Springer-Verlag, Berlin, Heidelberg, 1989, p. 150151.
24. FROMMER, A., AND SZYLD, D. B. An algebraic convergence theory for restricted additive schwarz methods using weighted max norms. *SIAM Journal on Numerical Analysis* 39, 2 (2002), 463–479.
25. GONDZIO, J., AND GROTHEY, A. Parallel Interior Point Solver for Structured Quadratic Programs: Application to Financial Planning Problems. *J. Annals of Operations Research* 152, 1 (2006), 319–339.
26. GONDZIO, J., AND SARKISSIAN, R. Parallel interior-point solver for structured linear programs. *Mathematical Programming* (2003).
27. GROSSMAN, I. *Global Optimization*. Springer, 2013.
28. GROSSMANN, I. E. Advances in mathematical programming models for enterprise-wide optimization. *Computers and Chemical Engineering* 47 (2012), 2–18.
29. GROTHEY, A., AND QIANG, F. PSMG-A Parallel Structured Model Generator for Mathematical Programming. Workingpaper, Optimization Online, 2014.

30. GUPTA, A., KARYPIS, G., AND KUMAR, V. Highly scalable parallel algorithms for sparse matrix factorization. *IEEE Transactions on Parallel and Distributed Systems* 8, 5 (1997), 502–520.
31. HALLAC, D., WONG, C., DIAMOND, S., SOSIC, R., BOYD, S., AND LESKOVEC, J. SnapVX: A Network-Based Convex Optimization Solver. *Journal of Machine Learning Research* 0 (2017), 1–5.
32. HART, W. E., LAIRD, C. D., WATSON, J.-P., WOODRUFF, D. L., HACKEBEIL, G. A., NICHOLSON, B. L., AND SIROLA, J. D. *Pyomo—optimization modeling in python*, second ed., vol. 67. Springer Science & Business Media, 2017.
33. HEO, S., RANGARAJAN, S., DAOUTIDIS, P., AND JOGWAR, S. S. Graph reduction of complex energy-integrated networks: Process systems applications. *AIChE Journal* (2014).
34. HIJAZI, H. L. Gravity : A mathematical modeling language for optimization and machine learning.
35. HÜBNER, J., SCHMIDT, M., AND STEINBACH, M. C. Optimization techniques for tree-structured nonlinear problems. *Computational Management Science* (2020).
36. HUCHETTE, J., LUBIN, M., AND PETRA, C. Parallel algebraic modeling for stochastic optimization. In *Proceedings of HPTCDL 2014: 1st Workshop for High Performance Technical Computing in Dynamic Languages - Held in Conjunction with SC 2014: The International Conference for High Performance Computing, Networking, Storage and Analysis* (2014).
37. JALVING, J., ABHYANKAR, S., KIM, K., HERELD, M., AND ZAVALA, V. M. A graph-based computational framework for simulation and optimisation of coupled infrastructure networks. *IET Generation, Transmission & Distribution* (2017), 1–14.
38. JALVING, J., CAO, Y., AND ZAVALA, V. M. Graph-based modeling and simulation of complex systems. *Computers & Chemical Engineering* 125 (2019), 134–154.
39. JALVING, J., AND ZAVALA, V. M. An optimization-based state estimation framework for large-scale natural gas networks. *Industrial & Engineering Chemistry Research* 57, 17 (2018), 5966–5979.
40. JIANG, W., QI, J., YU, J. X., HUANG, J., AND ZHANG, R. HyperX: A Scalable Hypergraph Framework. *IEEE Transactions on Knowledge and Data Engineering* (2018).
41. JOGWAR, S. S., RANGARAJAN, S., AND DAOUTIDIS, P. Reduction of complex energy-integrated process networks using graph theory. *Computers and Chemical Engineering* (2015).
42. KANG, J., CAO, Y., WORD, D. P., AND LAIRD, C. D. An interior-point method for efficient solution of block-structured NLP problems using an implicit Schur-complement decomposition. *Computers and Chemical Engineering* (2014).
43. KANG, J., CHIANG, N., LAIRD, C. D., AND ZAVALA, V. M. Nonlinear programming strategies on high-performance computers. In *Decision and Control (CDC), 2015 IEEE 54th Annual Conference on* (2015), IEEE, pp. 4612–4620.
44. KARYPIS, G., AND KUMAR, V. A Fast and High Quality Multilevel Scheme for Partitioning Irregular Graphs. *SIAM Journal on Scientific Computing* 20, 1 (1998), 359–392.
45. KARYPIS, G., AND KUMAR, V. Multilevel k-way hypergraph partitioning. In *Proceedings of the 36th Annual ACM/IEEE Design Automation Conference* (New York, NY, USA, 1999), DAC '99, ACM, pp. 343–348.
46. KIM, K., PETRA, C. G., AND ZAVALA, V. M. An asynchronous bundle-trust-region method for dual decomposition of stochastic mixed-integer programming. *SIAM Journal on Optimization* 29, 1 (2019), 318–342.
47. KIM, K., AND ZAVALA, V. M. Algorithmic innovations and software for the dual decomposition method applied to stochastic mixed-integer programs. *Mathematical Programming Computation* (2018).
48. KOUROUNIS, D., AND SCHENK, O. Structure-Exploiting Interior Point Methods.
49. LINDEROTH, J., AND WRIGHT, S. Decomposition algorithms for stochastic programming on a computational grid. *Computational Optimization and Applications* (2003).
50. LUBIN, M., PETRA, C. G., AND ANITESCU, M. The parallel solution of dense saddle-point linear systems arising in stochastic programming. *Optimization Methods and Software* (2012).
51. MAKHORIN, A. GNU Linear Programming Kit Version 4.32. <http://www.gnu.org/software/glpk/glpk.html>, 2000–2012.
52. MARAVELIAS, C. T. General framework and modeling approach classification for chemical production scheduling. *AIChE Journal* (2012).
53. MATSSON, S. E., ELMQVIST, H., AND OTTER, M. Physical system modeling with modelica. *Control Engineering Practice* 6, 4 (1998), 501–510.
54. MAYER, C., MAYER, R., BHOWMIK, S., EPPLE, L., AND ROTHERMEL, K. Hype: Massive hypergraph partitioning with neighborhood expansion. *2018 IEEE International Conference on Big Data (Big Data)* (2018), 458–467.
55. MOHARIR, M., KANG, L., DAOUTIDIS, P., AND ALMANSOORI, A. Graph representation and decomposition of ODE/hyperbolic PDE systems. *Computers and Chemical Engineering* (2017).
56. NEWMAN, M. E. Modularity and community structure in networks. *Proceedings of the National Academy of Sciences of the United States of America* (2006).
57. OSIADACZ, A. Simulation of transient gas flows in networks. *International Journal for Numerical Methods in Fluids* 4, 1 (1984), 13–24.
58. PAPA, D. A., AND MARKOV, I. L. Hypergraph partitioning and clustering. In *Handbook of Approximation Algorithms and Metaheuristics*. 2007.

59. PELLEGRINI, F. Distilling knowledge about scotch. In *Combinatorial Scientific Computing* (Dagstuhl, Germany, 2009), U. Naumann, O. Schenk, H. D. Simon, and S. Toledo, Eds., no. 09061 in Dagstuhl Seminar Proceedings, Schloss Dagstuhl - Leibniz-Zentrum fuer Informatik, Germany.
60. RAO, C. V., WRIGHT, S. J., AND RAWLINGS, J. B. Application of interior-point methods to model predictive control. *Journal of optimization theory and applications* 99, 3 (1998), 723–757.
61. RAWLINGS, J. B., AND MAYNE, D. *Model predictive control: Theory and design*, 2 ed. 2018.
62. REHFELDT, D., HOBBIE, H., SCHÖNHEIT, D., GLEIXNER, A. M., KOCH, T., AND MÖST, D. A massively parallel interior-point solver for linear energy system models with block structure.
63. RODRIGUEZ, J. S., LAIRD, C. D., AND ZAVALA, V. M. Scalable preconditioning of block-structured linear algebra systems using ADMM. *Computers and Chemical Engineering* 133 (2020), 106478.
64. SAHINIDIS, N. V., AND GROSSMANN, I. E. Convergence properties of generalized benders decomposition. *Computers and Chemical Engineering* (1991).
65. SCATTOLINI, R. Architectures for distributed and hierarchical Model Predictive Control - A review, 2009.
66. SCHLAG, S., HENNE, V., HEUER, T., MEYERHENKE, H., SANDERS, P., AND SCHULZ, C. k-way hypergraph partitioning via n -level recursive bisection. In *18th Workshop on Algorithm Engineering and Experiments, (ALENEX 2016)* (2016), pp. 53–67.
67. SCHLOEGEL, K., KARYPIS, G., AND KUMAR, V. *Graph Partitioning for High-Performance Scientific Simulations*. Morgan Kaufmann Publishers Inc., San Francisco, CA, USA, 2003, p. 491541.
68. SCHULZ, C., BAYER, S. K., HESS, C., STEIGER, C., TEICHMANN, M., JACOB, J., BERNARDES-LIMA, F., HANGU, R., AND HAYRAPETYAN, S. Course notes: Graph partitioning and graph clustering in theory and practice, 2015.
69. SETH BROMBERGER, J. F., AND OTHER CONTRIBUTORS. *Juliagraphs/lightgraphs.jl: an optimized graphs package for the julia programming language*, 2017.
70. SHIN, S., ANITESCU, M., AND ZAVALA, V. M. Overlapping schwarz decomposition for constrained quadratic programs, 2020.
71. SHIN, S., FAULWASSER, T., ZANON, M., AND ZAVALA, V. M. A parallel decomposition scheme for solving long-horizon optimal control problems. In *2019 IEEE 58th Conference on Decision and Control (CDC)* (2019), pp. 5264–5271.
72. SHIN, S., AND ZAVALA, V. M. Multi-grid schemes for multi-scale coordination of energy systems. In *Energy Markets and Responsive Grids*. Springer, 2018, pp. 195–222.
73. SHIN, S., AND ZAVALA, V. M. Multi-grid schemes for multi-scale coordination of energy systems. *Energy Markets and Responsive Grids* (2018).
74. SHIN, S., ZAVALA, V. M., AND ANITESCU, M. Decentralized schemes with overlap for solving graph-structured optimization problems. *IEEE Transactions on Control of Network Systems* (2020).
75. STEINBACH, M. C. Tree-sparse convex programs. *Mathematical Methods of Operations Research* (2003).
76. SUN, J., AND L, T. Dc optimal power flow formulation and solution using quadprogj, 2010.
77. TANG, W., ALLMAN, A., POURKARGAR, D. B., AND DAOUTIDIS, P. Optimal decomposition for distributed optimization in nonlinear model predictive control through community detection. *Computers & Chemical Engineering* 111 (2017), 43–54.
78. TANG, W., AND DAOUTIDIS, P. Network decomposition for distributed control through community detection in inputoutput bipartite graphs. *Journal of Process Control* (2018).
79. WACHTER, A., AND BIEGLER, L. T. On the implementation of an interior-point filter line-search algorithm for large-scale nonlinear programming. 25–57.
80. WANG, J., AND RALPHS, T. Computational Experience with Hypergraph-Based Methods for Automatic Decomposition in Discrete Optimization. In *Integration of AI and OR Techniques in Constraint Programming for Combinatorial Optimization Problems* (Berlin, Heidelberg, 2013), C. Gomes and M. Sellmann, Eds., Springer Berlin Heidelberg, pp. 394–402.
81. WATSON, J. P., WOODRUFF, D. L., AND HART, W. E. PySP: Modeling and solving stochastic programs in Python. *Mathematical Programming Computation* (2012).
82. ZAVALA, V. M. Stochastic optimal control model for natural gas networks. *Computers & Chemical Engineering* 64 (2014), 103–113.
83. ZAVALA, V. M. New Architectures for Hierarchical Predictive Control. *IFAC-PapersOnLine* 49, 7 (2016), 43–48.
84. ZENIOS, S. A. A distributed algorithm for convex network optimization problems. *Parallel Computing* 6 (1988), 45–56.
85. ZENIOS, S. A., AND PINAR, M. Parallel Block-Partitioning of Truncated Newton for Nonlinear Network Optimization. *SIAM Journal on Scientific and Statistical Computing* (1992).